

RESEARCH ARTICLE

10.1002/2014WR016102

Key Points:

- Abiotic controls are larger than biotic and are dominant in wet climates
- Hysteresis is stronger for Mediterranean than wet climates
- Heterogeneity in soil properties weakens signatures of hysteresis

Correspondence to:

S. Fatichi,
simone.fatichi@ifu.baug.ethz.ch

Citation:

Fatichi, S., G. G. Katul, V. Y. Ivanov, C. Pappas, A. Paschalis, A. Consolo, J. Kim, and P. Burlando (2015), Abiotic and biotic controls of soil moisture spatiotemporal variability and the occurrence of hysteresis, *Water Resour. Res.*, 51, 3505–3524, doi:10.1002/2014WR016102.

Received 5 JUL 2014

Accepted 4 APR 2015

Accepted article online 14 APR 2015

Published online 12 MAY 2015

Abiotic and biotic controls of soil moisture spatiotemporal variability and the occurrence of hysteresis

Simone Fatichi¹, Gabriel G. Katul^{2,3}, Valeriy Y. Ivanov^{1,4}, Christoforos Pappas¹, Athanasios Paschalis^{1,3}, Ada Consolo^{1,5}, Jongho Kim⁴, and Paolo Burlando¹

¹Institute of Environmental Engineering, ETH Zurich, Zürich, Switzerland, ²Department of Civil and Environmental Engineering, Duke University, Durham, North Carolina, USA, ³Nicholas School of the Environment, Duke University, Durham, North Carolina, USA, ⁴Department of Civil and Environmental Engineering, University of Michigan, Ann Arbor, Michigan, USA, ⁵Politecnico di Milano, Milan, Italy

Abstract An expression that separates biotic and abiotic controls on the temporal dynamics of the soil moisture spatial coefficient of variation $C_v(\theta)$ was explored via numerical simulations using a mechanistic ecohydrological model, Tethys-Chloris. Continuous soil moisture spatiotemporal dynamics at an exemplary hillslope domain were computed for six case studies characterized by different climate and vegetation cover and for three configurations of soil properties. It was shown that abiotic controls largely exceed their biotic counterparts in wet climates. Biotic controls on $C_v(\theta)$ were found to be more pronounced in Mediterranean climates. The relation between $C_v(\theta)$ and spatial mean soil moisture $\bar{\theta}$ was found to be unique in wet locations, regardless of the soil properties. For the case of homogeneous soil texture, hysteretic cycles between $C_v(\theta)$ and $\bar{\theta}$ were observed in all Mediterranean climate locations considered here and to a lesser extent in a deciduous temperate forest. Heterogeneity in soil properties increased $C_v(\theta)$ to values commensurate with field observations and weakened signatures of hysteresis at all of the studied locations. This finding highlights the role of site-specific heterogeneities in hiding or even eliminating the signature of climatic and biotic controls on $C_v(\theta)$, thereby offering a new perspective on causes of confounding results reported across field experiments.

1. Introduction

The importance of soil moisture on a multitude of processes related to hydrology, meteorology, ecology, and climate sciences [Grayson *et al.*, 1997; Porporato *et al.*, 2001; Ivanov *et al.*, 2004; Dirmeyer *et al.*, 2006; Seneviratne *et al.*, 2006, 2010; Legates *et al.*, 2011] is rarely disputed; however, the causes and explanations of its highly variable nature in space and time continues to draw significant research attention [Western and Blöschl, 1999; Famiglietti *et al.*, 1999; Katul *et al.*, 2007; Vereecken *et al.*, 2008; Robinson *et al.*, 2008; He *et al.*, 2014]. Studies that explored the major determinants of soil moisture spatiotemporal variability report climate, topography, soil, and vegetation as significant controls but differences in results hampered generalizations [Grayson *et al.*, 1997; Western *et al.*, 1999; Montaldo and Albertson, 2003; Wilson *et al.*, 2004; Choi *et al.*, 2007; Vanderlinden *et al.*, 2012]. More specifically, few studies [Teuling and Troch, 2005; Teuling *et al.*, 2007a; Gaur and Mohanty, 2013] separate quantitatively the importance of vegetation (biotic component) and physical factors (abiotic component) in controlling spatiotemporal patterns of soil moisture across different climates and vegetation types. Concurrently with analyses aimed at identifying external controls on soil moisture spatiotemporal variability, a series of studies also searched for temporal stability of soil moisture and/or correlations between the soil moisture spatial mean, $\bar{\theta}$ (at a given depth or vertically integrated) and the corresponding spatial variance, $\sigma^2(\theta)$, or coefficient of variation $C_v(\theta)$ [e.g., Grayson and Western, 1998; Choi and Jacobs, 2007; Brocca *et al.*, 2010, 2012]. Analyses of temporal stability of soil moisture were conceived to identify the sampling locations where soil moisture mean and temporal variability can be considered representative of a larger area (e.g., hillslope, transect, or catchment), reducing the need for extensive sampling [Vachaud *et al.*, 1985; Grayson and Western, 1998; Jacobs *et al.*, 2008; Cosh *et al.*, 2008; Hu *et al.*, 2010; Vanderlinden *et al.*, 2012; Martinez *et al.*, 2013]. Furthermore, the existence of a unique $C_v(\theta) - \bar{\theta}$ relation permits the estimation of the spatial variability of soil moisture from its mean value, thereby resembling a “closure” scheme in turbulence research [e.g., Mellor and Yamada, 1982]. Practical outcomes of such a closure is (i) to extend the use of remote sensing estimates of mean soil moisture to also characterize its spatial variability

[Famiglietti *et al.*, 1999; Crow *et al.*, 2005; Famiglietti *et al.*, 2008] and (ii) to account for spatial heterogeneities in modeling exercises [e.g., Pappas *et al.*, 2015]. Observations collected in the field generally support the idea of a negative correlation through an exponential or a linear function between $C_v(\theta)$ and $\bar{\theta}$ [Choi *et al.*, 2007; Brocca *et al.*, 2007; Teuling *et al.*, 2007b; Lawrence and Hornberger, 2007; Choi and Jacobs, 2007; Famiglietti *et al.*, 2008; Penna *et al.*, 2009; Tague *et al.*, 2010; Brocca *et al.*, 2010, 2012; Rosenbaum *et al.*, 2012], even though more complex patterns and hysteretic relations have been also found, especially in numerical experiments [Albertson and Montaldo, 2003; Teuling and Troch, 2005; Ivanov *et al.*, 2010; Vivoni *et al.*, 2010; Sela *et al.*, 2012; Martínez García *et al.*, 2014]. The hysteretic cycle has been attributed to the sequence of significant precipitation events with a wetting and homogenizing effect and to the subsequent lateral subsurface flow and evapotranspiration that impose a drying effect increasing heterogeneity when the domain is wet, and decreasing it as the domain becomes progressively drier [Ivanov *et al.*, 2010]. From theoretical considerations only, it is clear that in homogenous soils $C_v(\theta) - \bar{\theta}$ must decrease in the limiting cases of totally dry and wet conditions [Lawrence and Hornberger, 2007]. However, the dynamically interesting cases are in intermediate wetness states, as they often encompass the mode of soil moisture [Juang *et al.*, 2007].

As a starting point to link the controls on $C_v(\theta)$ to biotic and abiotic factors, the mechanisms that contribute to the generation and dissipation of the spatial variability of soil moisture are derived and explored. Hence, the objective is to use these variance budgets to explore the dependence of $C_v(\theta)$ on $\bar{\theta}$ for different climatic, vegetation, and soil types, so as to unfold biotic (vegetation) and abiotic controls (climate, soil properties) on $C_v(\theta)$. The goal of this analysis is to provide a mechanistic explanation on what dictates the shape and temporal evolution of the $C_v(\theta) - \bar{\theta}$ relation at the hillslope scale and understand how ubiquitous are the hysteretic relations found in earlier numerical studies that appear to be rarely supported by field measurements. The two main questions to be addressed here are: (i) what is the relative importance of biotic and abiotic controls on soil moisture spatiotemporal variability at the hillslope scale and across different environmental conditions? (ii) under what conditions is the relation between $C_v(\theta)$ and $\bar{\theta}$ hysteretic or unique?

Given the technical and economic challenges involved in addressing these questions using appropriate field data, numerical experiments that make use of a mechanistic ecohydrological model, Tethys-Chloris (T&C), are employed. However, we expect that the emergence of several soil moisture monitoring networks world-wide [Dorigo *et al.*, 2011, 2013; Gruber *et al.*, 2013] could potentially support or reject the hypotheses put forward in this study. T&C has been widely evaluated in previous studies for different vegetation types and climatic conditions [Fatichi *et al.*, 2012a, 2012b; Fatichi and Leuzinger, 2013; Fatichi *et al.*, 2014; Fatichi and Ivanov, 2014] and found to reproduce satisfactorily the hydrological and ecological state variables when forced by detailed meteorological inputs and boundary conditions. The numerical experiments are also expected to provide guidance in designing future soil moisture field campaigns and stimulating specific analyses in existing databases.

The current study is performed using a simple hillslope geometry with a characteristic shape that includes a central trough. The theoretical partition between abiotic and biotic controls contributing to soil moisture spatial variability is derived extending the previous studies of Katul *et al.* [1997] and Albertson and Montaldo [2003]. The outputs of the numerical model are then used with analytic expressions to partition the biotic and abiotic contributions to changes in $C_v(\theta)$ at the hillslope scale. Climate and vegetation boundary conditions derived for six eddy-covariance flux tower locations in the USA and Europe are used. The sensitivity of land-surface responses to homogeneous and heterogeneous soil textural properties is also evaluated.

2. Materials and Methods

2.1. Ecohydrological Model

Numerical simulations were carried out using the T&C model [Fatichi, 2010; Fatichi *et al.*, 2012a, 2012b; Fatichi and Leuzinger, 2013; Fatichi *et al.*, 2014; Fatichi and Ivanov, 2014]. T&C is a mechanistic distributed ecohydrological model intended to simulate essential components of hydrological and carbon cycle, resolving exchanges of energy, water, and CO_2 at the land surface and at the hourly time-scale. Mass and energy fluxes also control the temporal evolution of vegetation (carbon pools) that in turn can affect land-atmosphere exchanges through its biophysical structure and physiological properties. The simulation domain is represented by a regular grid as described by a digital elevation model. Topographic effects in controlling incoming radiation and lateral water transfers are explicitly accounted for. In each

computational element, vegetation biomass can occupy two vertical layers as a way of accommodating coexistence of trees and grasses. Horizontal composition of vegetation is also possible since each element can accommodate multiple species or plant functional types.

T&C solves shortwave and longwave radiation transfer through vegetation and accounts for aerodynamic, undercanopy, leaf boundary layer, stomatal, and soil resistances. The dynamics of the snow accumulation and melt are simulated by solving the energy balance of the snowpack. Snow interacts with vegetation since it can be intercepted by plants or fall to the ground, where it can be shaded. Soil moisture dynamics in saturated and unsaturated soils are solved using the one-dimensional Richards equation for vertical flow and the kinematic wave equation for lateral subsurface flow. As a result of infiltration and saturation excess mechanisms, water can pond on the surface or run off as overland flow. Channels and overland flows are solved through the kinematic wave approximation. Preferential flow dynamics associated with macropores or fingering flow are not addressed.

Photosynthesis is described at the leaf scale using conventional biochemical models [Farquhar *et al.*, 1980; Bonan *et al.*, 2011]. For the upscaling to the canopy level, sunlit and shaded leaves are treated separately in the computation of net assimilation and stomatal resistance that are also a function of other environmental conditions [Wang and Leuning, 1998]. An exponential decay of photosynthetic capacity is assumed, when upscaling photosynthesis from the leaf to the plant scale [Ivanov *et al.*, 2008; Bonan *et al.*, 2011]. The dynamics of seven carbon pools are simulated in the model and include (i) green aboveground biomass (leaves), (ii) living sapwood (for woody plants only), (iii) fine roots, (iv) carbohydrate reserve (nonstructural carbohydrates), (v) standing dead leaf biomass, (vi) fruit and flowers (representing reproduction cost), and (vii) heartwood and dead sapwood. The carbon assimilated through photosynthetic activity is then used for maintenance, growth, and reproduction, and it is lost in the process of respiration and tissue turnover. Carbon allocation and translocation are dynamically accounted for via resource availability (light and water), allometric constraints, and phenology. Organic matter turnover of the different carbon pools is simulated as a function of tissue longevity and environmental stresses, i.e., drought and low temperatures. Phenology is modeled by considering four states [Arora and Boer, 2005]: dormant, maximum growth, normal growth, and senescence. Forest demography and nutrient dynamics are neglected in current calculations, which implies that the vegetation is at a mature phase and in equilibrium with its nutritional environment. A detailed description of the model structure and process parameterizations is presented elsewhere [Fatichi *et al.*, 2012a].

2.2. Climate Forcing and Vegetation

Six locations corresponding to sites of eddy-covariance flux towers with different climate and vegetation cover conditions distributed across the USA and Europe are selected to perform the numerical experiments. A broad range of climate and vegetation types allow the investigation of differences and similarities in the spatiotemporal dynamics of soil moisture as well as in the magnitude of biotic versus abiotic controls. The six analyzed locations are: (i) Rietholzbach (47.37°N, 8.99°E; elevation 754 m a.s.l.), a grassland located in subalpine Switzerland [Teuling *et al.*, 2010; Seneviratne *et al.*, 2012; Fatichi *et al.*, 2014]; (ii) Davos (46.81°N, 9.85°E; elevation 1639 m a.s.l.), an evergreen spruce forest in the eastern Alps of Switzerland [Etzold *et al.*, 2011; Churakova (Sidorova) *et al.*, 2014]; (iii) the University of Michigan Biological Station, UMBS (45.55°N, 84.71°W; elevation 234 m a.s.l.), a mixed deciduous forest in the north of the lower Michigan peninsula [Curtis *et al.*, 2005; Gough *et al.*, 2009, 2013; He *et al.*, 2013, 2014]; (iv) San Rossore (43.72°N, 10.28°E; elevation 4 m a.s.l.), a Mediterranean evergreen needleleaf forest composed of maritime pine and stone pine located in central Italy [Tirone, 2003; Chiesi *et al.*, 2007]; (v) Vaira ranch (38.41°N, 120.95°W; elevation 129 m a.s.l.), a "California, annual grassland" dominated by C₃ species, located near Lone, California [Baldocchi *et al.*, 2004; Xu and Baldocchi, 2004; Ma *et al.*, 2007; Ryu *et al.*, 2008]; and (vi) Lucky Hills (31.44°N, 110.30°W; elevation 1372 m a.s.l.), a sparse shrub community, represented by both evergreen (creosote bush), and deciduous shrubs (whitethorn acacia) located near Tombstone in the south-east Arizona [Emmerich and Verdugo, 2008; Keefer *et al.*, 2008]. The major climatic and land cover characteristics as well as the simulation period, 5 years for all of the locations, are summarized in Table 1. The seasonality of precipitation and energy forcings is shown in Figure 1. A full vegetation cover is assumed for five locations, while homogenous but sparse vegetation cover is assumed for Lucky Hills with a vegetation fraction set to 0.35 in each element of the domain. A description of the edaphic conditions, as well as species composition for these six locations can be found elsewhere [Fatichi *et al.*, 2012b, 2014; Fatichi and Ivanov, 2014] along with all model parameters for four out of the six sites. Specifically, the performance of T&C has been previously presented for the Swiss grasslands

Table 1. Site Characteristics as Inferred From Observed Data and Integrated in the Distributed Domain

	Rietholzbach (CH)	Davos (CH)	UMBS (MI)	San Rossore (IT)	Vaira ranch (CA)	Lucky Hills (AZ)
Period	Jan 2001–Dec 2005	Jan 2000–Dec 2004	Jan 1999–Dec 2003	Jan 2001–Dec 2005	Nov 2000–Oct 2005	Jul 1996–Jun 2001
Land Cover	Grass	Evergreen needleleaves	Deciduous broadleaves	Evergreen needleleaves	Grass	Shrubs mixed
Mean P_r (mm yr ⁻¹)	1395	938	899	914	516	499
Mean T_a (°C)	8.0	2.6	7.0	15.3	15.7	16.8
Mean R_{sw} (W m ⁻²)	134	157	151	172	218	251
Mean VPD (Pa)	321	297	395	401	1007	1329
Sim. ET (mm yr ⁻¹)	664	411	711	723	422	454
Sim. GPP (gC m ⁻² yr ⁻¹)	1950	1114	1162	1832	893	189

^aThe first year of simulation is excluded from the analysis and treated as a spin-up period. P_r (mm yr⁻¹) is the annual precipitation, T_a (°C) is the air temperature, R_{sw} (W m⁻²) is the shortwave radiation, VPD (Pa) is the vapor pressure deficit, ET (mm yr⁻¹) is the simulated evapotranspiration with homogenous soil properties, and GPP (gC m⁻² yr⁻¹) is the simulated Gross Primary Production with homogenous soil properties.

and Rietholzbach [Fatichi et al., 2014], Lucky Hills [Fatichi et al., 2012a, 2012b], and Vaira ranch and the UMBS [Fatichi and Ivanov, 2014]. Model results in terms of energy, carbon fluxes, soil moisture and temperature, and vegetation dynamics (e.g., Leaf Area Index, LAI) agree well with independent measurements at the four sites. Similar model performance has been obtained comparing model simulations with flux tower observations for the locations of Davos and San Rossore.

2.3. Hillslope Domain and Boundary Conditions

The domain used for the numerical experiments corresponds to the hillslope of the Biosphere 2 experiment [Huxman et al., 2009]. This hillslope represents a zero-order basin with uniform soil depth of 1 m (normal to the surface) and a characteristic convex shape with a central hollow that imposes three-dimensional controls on water flow. The hillslope size is 15 m × 30 m with an average slope of 10.5°. Because of its uniformity and structural simplicity, this hillslope has been previously used for modeling purposes [Hopp et al., 2009; Ivanov et al., 2010; Kim and Ivanov, 2014]. The computational domain is discretized into a regular grid of 1 m × 1 m in the horizontal and with 12 layers of increasing depth in the vertical, from 1 cm near the surface to 20 cm near the bottom. Impermeable boundary conditions were forced for the upstream and lateral hillslope faces and for its bottom, which are consistent with the Biosphere 2 experiment. Three soil configurations with vertically homogenous hydraulic properties were used in the model runs. The first corresponds to a homogenous loamy soil across the entire hillslope composed of 40% sand, 37.5% silt, 20% clay, and with a 2.5% organic content. The second corresponds to vertically homogenous but laterally heterogeneous soil conditions. Specifically, a random field with the sand content uniformly distributed between 28 and 52%, silt between 19.5 and 55.5%, and clay between 14 and 26% was generated (the organic content was kept constant at 2.5%). The range of sand and clay contents was chosen to depart ±30% from the pure loam textural properties. The random field of soil composition was assumed to be spatially uncorrelated. This assumption was necessary given the small size of the hillslope (15 m × 30 m), which cannot accommodate observed correlation lengths [Western et al., 1998, 2004]. The third configuration intentionally amplifies spatial heterogeneity in soil composition above its common state by imposing a random field where each cell has texture with sand content defined as a uniformly distributed variate between 10 and 90%, silt between 0 and 82.5%, and clay between 5 and 50%, with a constraint to 97.5% on the sum of the three (i.e., organic content was assumed constant as in the other cases). This third soil configuration spans different soil textural types from sandy to clay soils and, while unrealistic for a small hillslope, it is intended to magnify the role of local soil heterogeneity. Pedotransfer functions were then used to convert soil textural characteristics into soil hydraulic parameters when computing hydraulic conductivity and soil water retention curves [Saxton and Rawls, 2006]. From this conversion, the spatial C_v of saturated and residual water content, and saturated hydraulic conductivity are 0.016, 0.175, and 0.294, respectively, for the second soil configuration (heterogeneous loam) and 0.050, 0.493, and 1.088, for the third soil configuration (fully heterogeneous soil). A more conventional metric, the standard deviation of the natural logarithm of the saturated hydraulic conductivity, is 0.286 for the second and 1.231 for the third soil configuration.

2.4. Partitioning Biotic and Abiotic Controls

The contributions of biotic and abiotic factors on temporal changes in $C_v(t)$ are quantified through covariances of different water balance terms and soil moisture at the hillslope scale. This derivation follows

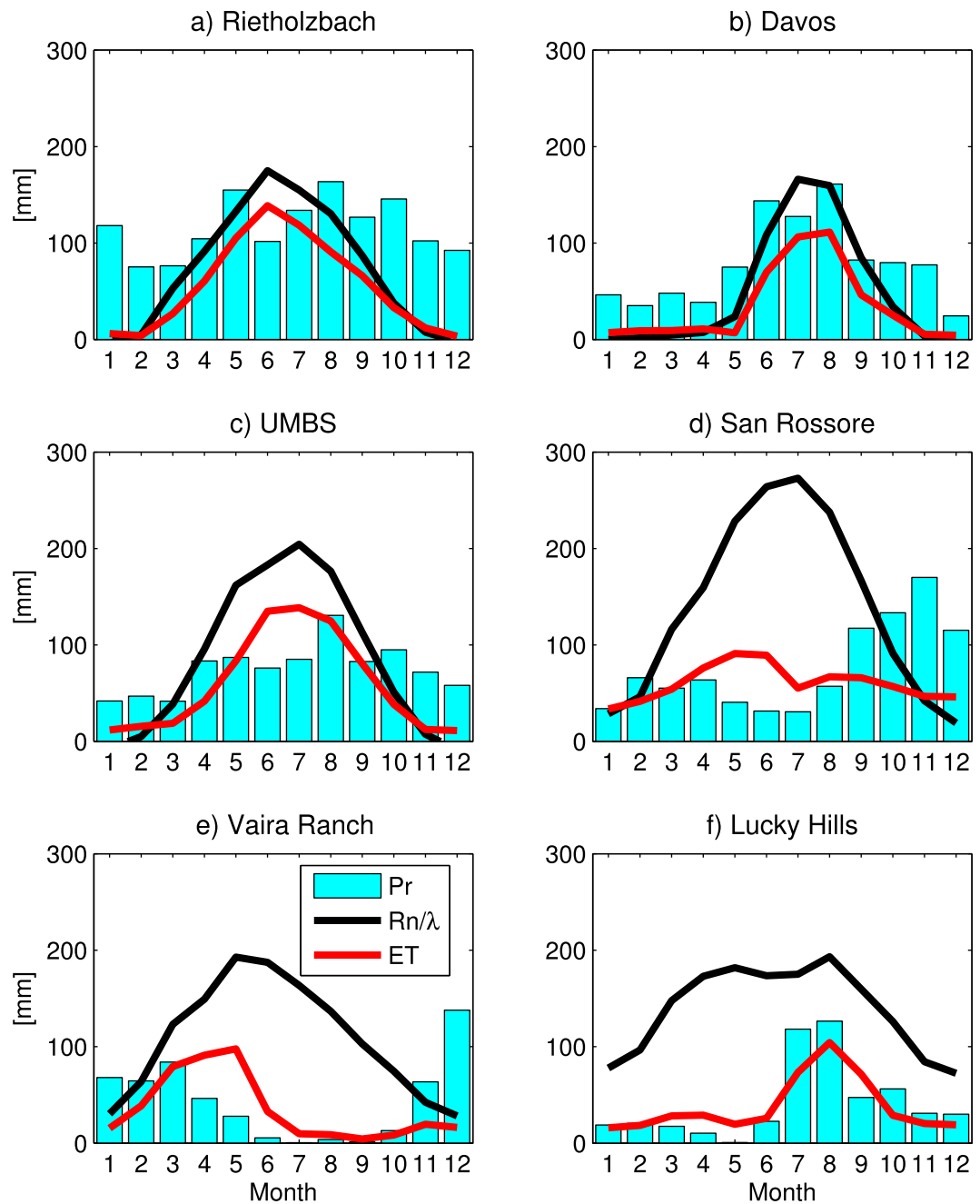


Figure 1. Seasonality of observed precipitation (Pr) and simulated evapotranspiration (ET) and net radiation divided by the latent heat of vaporization (R_n/λ) for the six analyzed locations.

closely previous work of *Katul et al.* [1997] and *Albertson and Montaldo* [2003] who obtained budget equations for the time evolution of spatial variance of soil moisture, $\sigma^2(\theta)$.

The instantaneous but vertically integrated soil moisture budget at a given computational element in T&C is given by:

$$Z_s \frac{\partial \theta}{\partial t} = f - E_g - T_H - T_L - L_k + Q_{l,in} - Q_{l,out} - R_d, \tag{1}$$

where Z_s (mm) is the soil depth, θ (-) is vertically integrated soil moisture content, f (mm h^{-1}) is actual infiltration, E_g (mm h^{-1}) is ground evaporation, T_H (mm h^{-1}) is transpiration from high vegetation, T_L (mm h^{-1}) is transpiration from low vegetation, L_k (mm h^{-1}) is leakage from soil to bedrock, $Q_{l,in}$ (mm h^{-1}) is

vertical integrated incoming lateral flow, $Q_{l,out}$ (mm h^{-1}) is vertical integrated outgoing lateral flow, and R_d (mm h^{-1}) is saturation excess runoff. The time evolution of the spatial mean (indicated by overbar) can be obtained as the spatial average of equation (1):

$$Z_s \frac{\partial \bar{\theta}}{\partial t} = \bar{f} - \bar{E}_g - \bar{T}_H - \bar{T}_L - \bar{L}_k + \bar{Q}_{l,in} - \bar{Q}_{l,out} - \bar{R}_d. \tag{2}$$

Using Leibniz’s theorem, spatial averaging commutes with the differential operator here because the spatial boundaries do not evolve in time. A budget equation for the instantaneous spatial fluctuations in soil moisture can now be derived by subtracting the spatially averaged from the instantaneous equation to yield:

$$Z_s \frac{\partial \theta'}{\partial t} = f' - E'_g - T'_H - T'_L - L'_k + Q'_{l,in} - Q'_{l,out} - R'_d, \tag{3}$$

where the deviations from the spatial mean are defined by primes representing $\theta' = \theta - \bar{\theta}$, $f' = f - \bar{f}$, $E'_g = E_g - \bar{E}_g$, etc. Multiplying equation (3) by $2\theta'$ and applying the “spatial average” operator, a budget equation for the dynamics of the soil moisture spatial variance can be derived and is given by:

$$Z_s \frac{\partial \overline{\theta'^2}}{\partial t} = 2\overline{\theta' f'} - 2\overline{\theta' E'_g} - 2\overline{\theta' T'_H} - 2\overline{\theta' T'_L} - 2\overline{\theta' L'_k} + 2\overline{\theta' Q'_{l,in}} - 2\overline{\theta' Q'_{l,out}} - 2\overline{\theta' R'_d}. \tag{4}$$

Using equation (4), one can partition the contributions of the different components to the temporal evolution of the spatial variance into biotic and abiotic. Specifically, if we denote $B_{var} = \frac{2}{Z_s} (\overline{\theta' T'_H} + \overline{\theta' T'_L})$ and $A_{var} = \frac{2}{Z_s} (\overline{\theta' f'} - \overline{\theta' E'_g} - \overline{\theta' L'_k} + \overline{\theta' Q'_{l,in}} - \overline{\theta' Q'_{l,out}} - \overline{\theta' R'_d})$, we obtain the partition between biotic B_{var} and abiotic A_{var} factors of the time derivative of the spatial variance of soil moisture:

$$\frac{\partial \overline{\theta'^2}}{\partial t} = A_{var} - B_{var}. \tag{5}$$

A partition between biotic B_μ and abiotic A_μ contributions to changes in the mean field can be similarly derived, where $A_\mu = \frac{1}{Z_s} (\bar{f} - \bar{E}_g - \bar{L}_k + \bar{Q}_{l,in} - \bar{Q}_{l,out} - \bar{R}_d)$, and $B_\mu = \frac{1}{Z_s} (\bar{T}_H + \bar{T}_L)$, which is:

$$\frac{\partial \bar{\theta}}{\partial t} = A_\mu - B_\mu. \tag{6}$$

Consequently, the time evolution of the spatial coefficient of variation can now be written as:

$$\frac{\partial C_v}{\partial t} = \frac{\partial \left(\frac{\sqrt{\overline{\theta'^2}}}{\bar{\theta}} \right)}{\partial t} = \frac{\frac{\partial \sigma}{\partial t} \bar{\theta} - \frac{\partial \bar{\theta}}{\partial t} \sigma}{\bar{\theta}^2}, \tag{7}$$

where $\sigma = \sqrt{\overline{\theta'^2}}$ is the spatial standard deviation. It follows that:

$$\frac{\partial C_v}{\partial t} = \frac{1}{\bar{\theta}} \left(\frac{\partial \sigma}{\partial t} - \frac{\partial \bar{\theta}}{\partial t} C_v \right), \tag{8}$$

but $\frac{\partial \sigma}{\partial t}$ can be written as:

$$\frac{\partial \sigma}{\partial t} = \frac{1}{2\sqrt{\overline{\theta'^2}}} \frac{\partial \overline{\theta'^2}}{\partial t}, \tag{9}$$

therefore:

$$\frac{\partial C_v}{\partial t} = \frac{1}{\bar{\theta}} \left(\frac{1}{2\sqrt{\overline{\theta'^2}}} (A_{var} - B_{var}) - C_v (A_\mu - B_\mu) \right). \tag{10}$$

Separating the biotic from the abiotic components results in:

$$\frac{\partial C_v}{\partial t} = \frac{1}{2\bar{\theta}\sqrt{\overline{\theta'^2}}} A_{var} - \frac{C_v}{\bar{\theta}} A_\mu + \frac{C_v}{\bar{\theta}} B_\mu - \frac{1}{2\bar{\theta}\sqrt{\overline{\theta'^2}}} B_{var}, \tag{11}$$

where the first two terms of equation (11) represent the abiotic controls and the second two terms the biotic controls. Note that if C_v is assumed to change in time slower than the other quantities, we can derive a steady state solution, i.e., $\frac{\partial C_v}{\partial t} = 0$:

$$C_v = \frac{\frac{1}{2\sqrt{\bar{\theta}^2}}(A_{var} - B_{var})}{A_\mu - B_\mu} \quad (12)$$

Equation (12) suggests the occurrence of different $C_v - \bar{\theta}$ trajectories for changes in the hydrological forcing as a function of the spatial standard deviation of soil moisture $\sqrt{\bar{\theta}^2}$, and therefore the occurrence of hysteretic relations. Finally, equation (11) can be re-casted as:

$$\frac{\partial C_v}{\partial t} = T_1 + T_2 + T_3 + T_4, \quad (13)$$

where $T_1 = -\frac{C_v}{\bar{\theta}} A_\mu$ is the abiotic control due to changes in the mean, $T_2 = \frac{1}{2C_v \bar{\theta}^2} A_{var}$ is the abiotic control due to changes in the variance, $T_3 = \frac{C_v}{\bar{\theta}} B_\mu$ is the biotic control due to changes in the mean, and $T_4 = -\frac{1}{2C_v \bar{\theta}^2} B_{var}$ is the biotic control due to changes in the variance. The four T terms are all positive when they create heterogeneity, and they are negative when their contribution is toward homogenization of the spatial soil moisture field.

The four terms on the right side of equation (13) can be computed directly at each time step because all quantities are explicitly resolved in T&C. The numerical scheme is checked by comparing results for the right and left hand side of equation (13). The differences were two orders of magnitude smaller than the terms themselves suggesting adequate accuracy in the numerical solution.

2.5. Design of the Numerical Experiments

Using meteorological time series as forcing inputs and vegetation properties for each of the selected locations, continuous model runs were conducted at the hourly time scale for a 5 year period (Table 1) using the Biosphere 2 hillslope domain. The model runs are presented for the three soil configurations described above: (i) homogenous loam, (ii) heterogeneous loam, and (iii) fully heterogeneous soil. The first year of simulation was discarded to avoid initialization issues in the three-dimensional distribution of soil moisture. Model runs with locally observed soil textural properties were carried out for all six sites but are not discussed here because the specific objective of this study is to separate the effects of climate and vegetation from soil textural properties on the spatiotemporal dynamics of soil moisture. Additional simulations were also carried out by increasing soil depth to 3 m and decreasing it to 0.6 m, as well as relaxing the assumption of an impermeable bottom (replaced with a free drainage condition). It was found that these results were of limited additional value when compared to the basic cases and are only briefly mentioned in the discussion.

All of the fluxes and states mentioned in section 2.4, i.e., $\bar{\theta}$, $C_v(\theta)$ and T_1 , T_2 , T_3 , and T_4 are computed by the T&C model. To provide a quantitative description of hysteresis in the $C_v(\theta) - \bar{\theta}$ space, a hysteresis index HY_I was defined as:

$$HY_I = 100 \frac{\int \Delta(C_v) d\bar{\theta}}{[\max(C_v) - \min(C_v)]}, \quad (14)$$

where $\Delta(C_v)$ is the difference between the maximum and minimum $C_v(\theta)$ in a given interval of mean soil moisture $d\bar{\theta}$, while $\max(C_v)$ and $\min(C_v)$ are the extrema of $C_v(\theta)$. The index HY_I measures hysteresis because it computes the envelope area of the points in the $C_v(\theta) - \bar{\theta}$ domain, divided by the maximum variability in $C_v(\theta)$. Larger values of HY_I denote a stronger hysteretic relation.

3. Results

3.1. Hydrological Processes Affecting Hillslope Soil Moisture Variability

Before analyzing long-term dynamics of space-time soil moisture variability, we discuss how the four terms of equation (13) are controlled by the various hydrological processes. To highlight specific climatic or

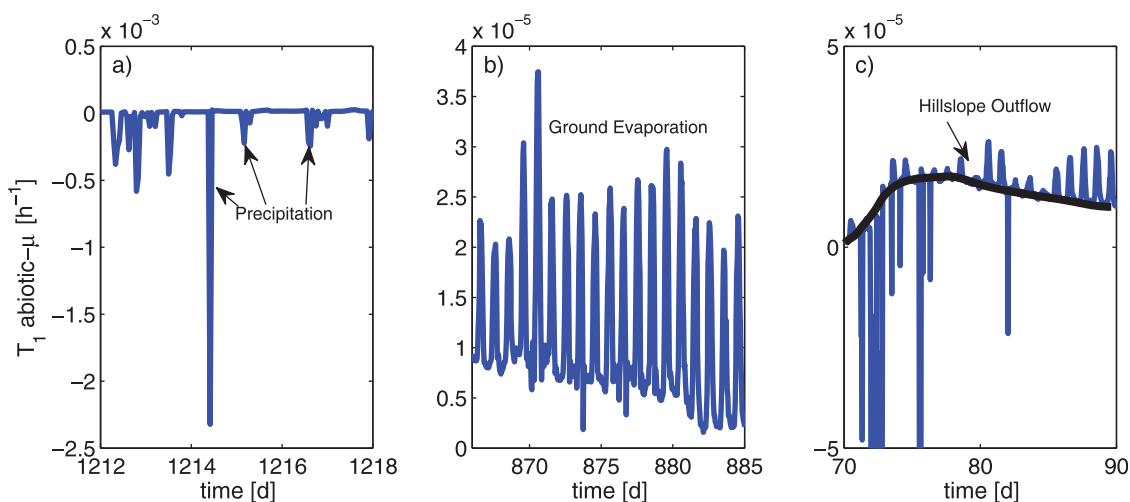


Figure 2. Exemplary periods highlighting the main processes controlling the term T_1 , which represents the abiotic controls on the soil moisture spatial mean. (a) Precipitation; (b) ground evaporation, and (c) hillslope outflow. Simulations are extracted from the Vaira ranch case study with homogenous soil conditions (the black line highlights the effect of hillslope outflow only).

hydrologic controls, periods of few days or weeks during which the role of a specific process (e.g., precipitation, transpiration) is dominant over the others are extracted from simulations of Vaira ranch and referenced to the homogenous soil conditions.

The first term T_1 represents abiotic controls on the soil moisture mean. This is a simple case to analyze because water input to the hillslope as precipitation provides a homogenizing effect (T_1 is negative), increasing the mean soil moisture and therefore reducing C_v (Figure 2). Ground evaporation and water outflow from the hillslope domain as subsurface flow or runoff have the opposite effect, with a positive T_1 , i.e., decreasing the mean and increasing C_v (Figure 2).

The second term T_2 represents the abiotic controls on the soil moisture variance. In response to precipitation events that are assumed spatially uniform over the hillslope, T_2 typically assumes negative values imposing a homogenizing effect over the domain (Figure 3a). This is the case when antecedent moisture conditions are not particularly dry. Conversely, in the case of dry initial state a precipitation event creates heterogeneity, e.g., T_2 is positive (Figure 3b). This can be the result of at least three factors, a spatially variable infiltration capacity, rain interception and throughfall, and hillslope geometry. Rainfall is assumed to fall in the vertical direction, but infiltration and soil moisture are computed in the direction normal to the ground surface. Consequently, steeper locations receive less rain per unit area and remain relatively drier than flat areas even for the same amount of vertical rainfall because they have a larger volume to fill. Additional processes affecting T_2 are ground evaporation and lateral subsurface water fluxes. Ground evaporation mostly contributes to the production of soil moisture variance, even though with absolute values smaller than those for precipitation (Figure 3c). Lateral fluxes, which mostly occur as a consequence of saturation at the impermeable boundary, follow topographic gradients and contribute to creating heterogeneity delivering moisture into the trough (Figure 3d).

The third term T_3 , the biotic control on the mean, is always positive. T_3 is simply the result of transpiration that extracts water from the system and therefore, increases C_v (Figure 4a). More interesting are the temporal dynamics of T_4 , which represents the biotic controls on the soil moisture variance. The process affecting T_4 is transpiration but T_4 can be positive (enhancing variability), in mild to wet conditions, and negative (suppressing variability), when the average soil moisture decreases (Figure 4b). In wet conditions, this behavior can be explained because transpiration is energy limited, and hence, any spatial variability in net radiation due to hillslope geometry and vegetation adds variance. As the hillslope dries, the sign of T_4 changes because certain areas become water limited, while others are still energy limited. Larger transpiration fluxes from wet areas homogenize soil moisture distribution throughout the hillslope. In this second condition, the magnitude of T_4 is typically much larger. The switch in T_4 sign is evident for locations with Mediterranean climate (San Rossore and Vaira ranch) and it occurs every summer, while it is rare and confined to the most extreme dry events for the Swiss locations (Rietholzbach and Davos).

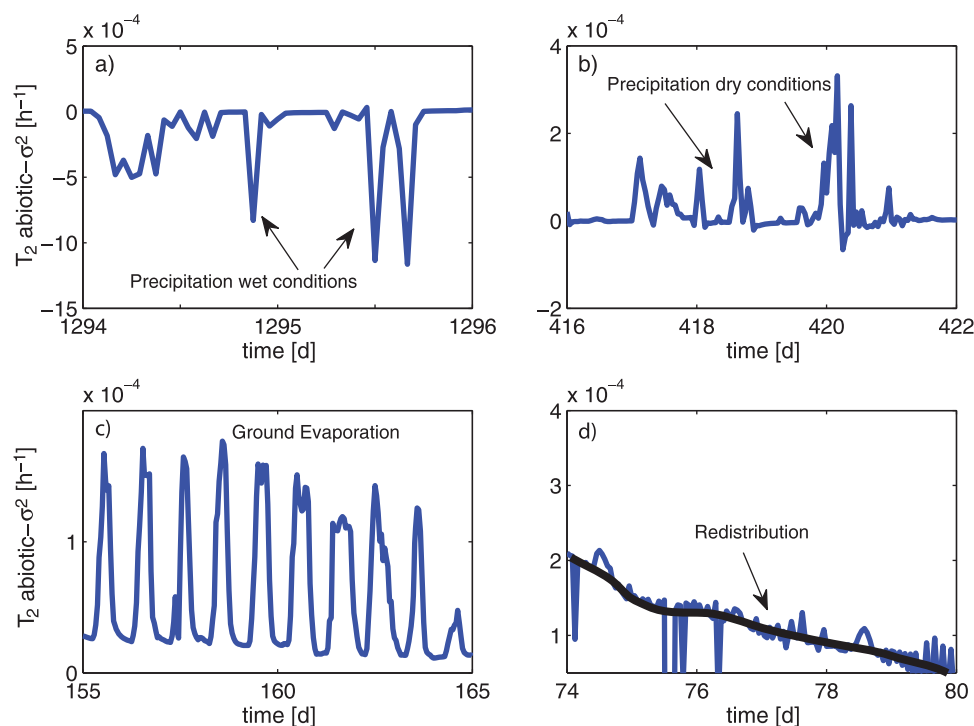


Figure 3. Exemplary periods highlighting the main processes controlling the term T_2 , which represents abiotic controls on the soil moisture spatial variance. (a) Precipitation in wet conditions; (b) precipitation in dry conditions; (c) ground evaporation, and (d) lateral water redistribution. Simulations are extracted from the Vaira ranch case study with homogenous soil conditions (the black line highlights the effect of lateral water redistribution only).

3.2. Soil Moisture Dynamics: Homogenous Soil

In order to illustrate the relative importance of biotic and abiotic contributions to $\frac{\partial C_v}{\partial t}$, we selected colored markers between 0 (fully abiotic controlled) and 1 (fully biotic controlled) in the diagram that relates the mean soil moisture $\bar{\theta}$ to its spatial coefficient of variation $C_v(\theta)$ for each hour (Figure 5). The diagram is a phase space representation of hydrological dynamics affecting soil moisture mean and spatial distribution. Using homogenous loamy soil, the relation between $C_v(\theta)$ and $\bar{\theta}$ is almost unique and dominated by abiotic controls for the two Swiss locations (Rietholzbach and Davos), with higher $C_v(\theta)$ as the hillslope water content decreases (Figure 5). An exception is represented by the extremely dry summer of 2003 in Europe [Leuzinger *et al.*, 2005; Granier *et al.*, 2007], where biotic factors become dominant, decreasing $C_v(\theta)$ for low $\bar{\theta}$, more evident for Rietholzbach. The transition between abiotic and biotic controls is rather smooth but biotic contributions to $\frac{\partial C_v}{\partial t}$ rarely exceeds 0.5. The presence of persistent winter snow cover in Davos “freezes” the system state for a long duration in specific conditions of $C_v(\theta)=0.09$ and $\bar{\theta}=0.36$ (corresponding roughly to the field capacity), as can be observed from the histogram of $C_v(\theta)$.

Conversely, the locations with a Mediterranean climate (San Rossore and Vaira ranch) show a pronounced hysteretic cycle that follows seasonality of climate and vegetation, which are out of phase for these two case studies. Abiotic controls during the winter season increase $C_v(\theta)$. Biotic controls in late winter and spring become progressively significant. When they attain a dominant role, soil moisture variability starts to decrease and reaches an “attractor state” characterized by low soil moisture but low spatial variability. These conditions (the “attractor state”) represent about 15% and 40% of the time for San Rossore and Vaira ranch respectively, as can be observed from the histograms of $C_v(\theta)$ and $\bar{\theta}$. Rainfall events after a dry season contribute to increase of $\bar{\theta}$ but $C_v(\theta)$ still remains small until a critical $\bar{\theta}$ threshold (close to field capacity of $\theta \approx 0.36$) is exceeded. At this stage, water saturation occurs at the soil-bedrock interface and lateral redistribution occurs [see also Ivanov *et al.*, 2010]. The hysteretic cycle is repeated each year. A maximum in $C_v(\theta)$ corresponds to the change in sign of T_4 , the biotic controls on the soil moisture variance, and characterizes the water content ($\theta \approx 0.20-0.25$) at which the hillslope starts to be water limited which is also a function of the vegetation type and properties. After this time point in the hillslope drying, T_3 and T_4 exert to a strong homogenizing effect.

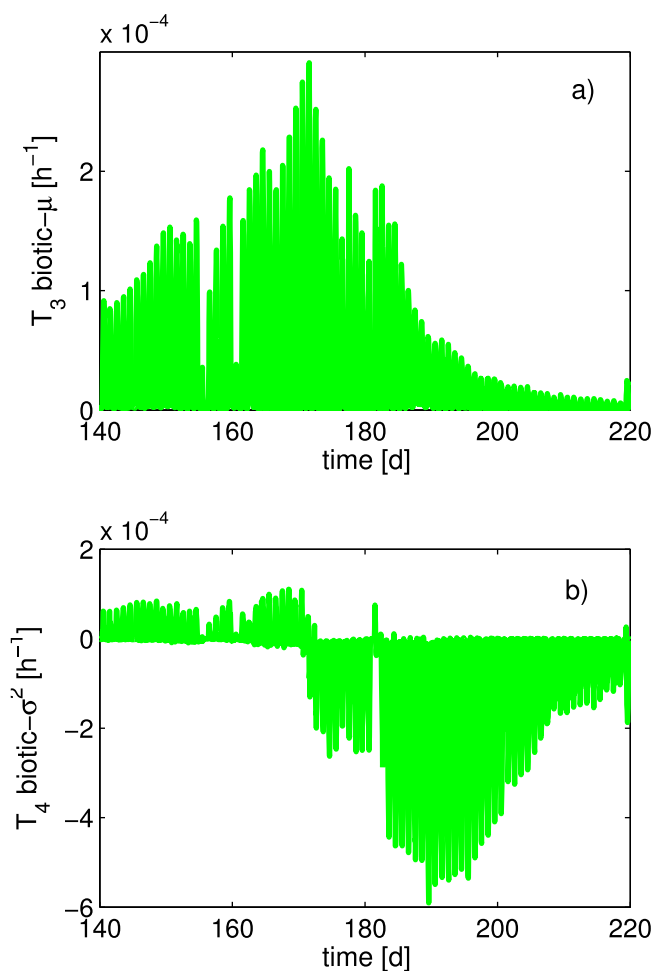


Figure 4. Exemplary periods highlighting the main processes controlling the term T_3 , which represents the biotic control on the soil moisture mean (subplot a) and T_4 , which represents the biotic controls on the soil moisture variance (subplot b). Simulations are extracted from the Vaira ranch case study with homogenous soil conditions.

3.3. Soil Moisture Dynamics: Heterogeneous Soil

Introducing spatially heterogeneous soil composition leads to a decrease in the occurrence of hysteresis in the $C_v(\theta)$ - $\bar{\theta}$ relation. This is already evident from the runs associated with the second soil configuration (Figure 6, heterogeneous loam) and becomes more evident for the third soil configuration (Figure 7, fully heterogeneous soil), which eliminates hysteresis altogether. For these heterogeneous soil conditions (Figure 7), the relation between $C_v(\theta)$ and $\bar{\theta}$ becomes unique, with $C_v(\theta)$ increasing linearly, in wet conditions, or exponentially for drier soils and for all of the presented case studies. In other words, even though the same physical processes described for homogenous soil are occurring, soil moisture patterns remain heterogeneous at the dry end of the range of soil moisture due to the spatial variability in hydraulic properties. The magnitude of $C_v(\theta)$ increases substantially, when transitioning from homogenous loam, to heterogeneous loam, and to fully heterogeneous soil conditions. The transition between the abiotic and biotic controls with decreasing $\bar{\theta}$ is maintained but less smooth than for homogenous soil conditions (Figures 6 and 7). The long-term partition of precipitation between evapotranspiration and hillslope outflow is only marginally affected by the heterogeneity in soil properties (Table 2), except for the semi-arid location where runoff, mostly as a consequence of soil-sealing effects, increases for heterogeneous soil properties, which is in agreement with the previous studies [Saghafian et al., 1995; Assouline and Mualem, 2006].

The location of the UMBS shows signs of hysteretic behavior but much less pronounced when compared to the two sites with a Mediterranean climate. Precipitation at the UMBS is rather uniform throughout the year, which prevents the system from reaching the attractor state (low $C_v(\theta)$ and $\bar{\theta}$). The system is characterized by frequent cycles of wetting and redistribution events during the growing season. Multiple “scanning curves” are the result of overlap between the biotic and abiotic effects, increasing variability (transpiration and lateral redistribution) and abiotic homogenization (rainfall). The transition between abiotic and biotic controls with decreasing $\bar{\theta}$ is evident, even though biotic controls are rarely dominant (≥ 0.7). Finally, the semiarid climate of Lucky-Hills constrains the system to be within the attractor state most of the time, with a mixed effect of biotic and abiotic controls. In the simulated period, only one significant rainfall event triggered lateral redistribution of water and traces a hysteretic cycle. It is to be noted that a much less frequent redistribution with comparison to the experiment of Ivanov et al. [2010] is a result of different soil textural properties.

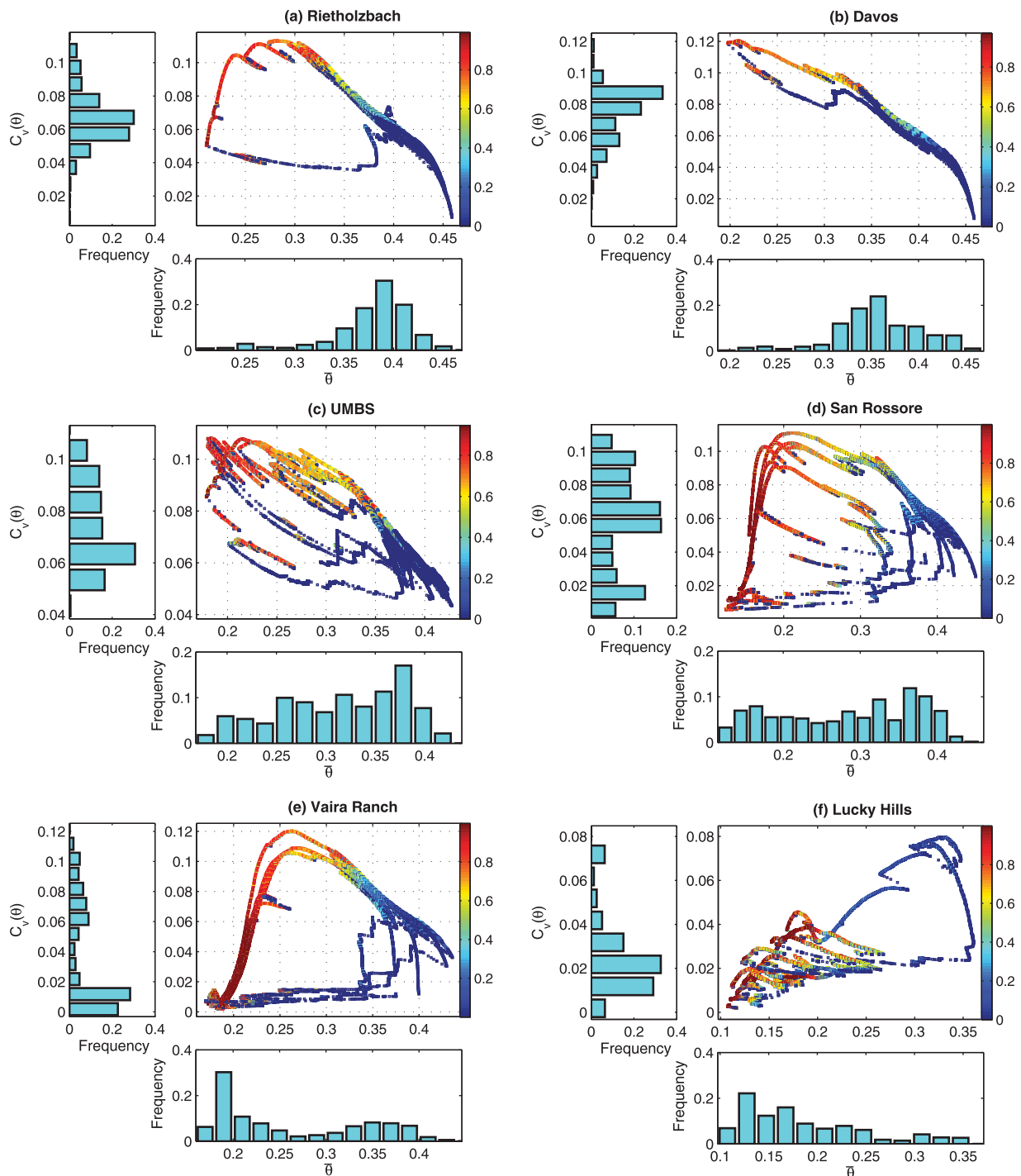


Figure 5. The coefficient of variation of depth-integrated soil moisture content $C_v(\theta)$ as a function of its mean hourly value $\bar{\theta}$ obtained using the **first** soil configuration (homogenous loam) for the case studies of (a) Rietholzbach, (b) Davos, (c) UMBS, (d) San Rossore, (e) Vaira ranch, and (f) Lucky Hills. The histograms of $C_v(\theta)$ and $\bar{\theta}$ are also illustrated. The color bars indicate for each hour the absolute proportion between biotic controls and abiotic controls scaled between 0 (fully abiotic controlled) and 1 (fully biotic controlled), i.e., $(|T_3|+|T_4|)/(|T_1|+|T_2|+|T_3|+|T_4|)$.

More quantitatively, the dissipation of hysteresis in the $C_v(\theta)-\bar{\theta}$ relation with increasing soil heterogeneity is evident from a decrease in the hysteresis index HY_I with larger variability in soil hydraulic properties exemplified by the coefficient of variation of the saturated hydraulic conductivity $C_v(K_{sat})$ (Figure 8). Similar patterns are obtained using the C_v of saturated and residual water content (not shown). There is a threefold to fourfold decrease in HY_I when transitioning from homogenous loam to fully heterogeneous soil conditions

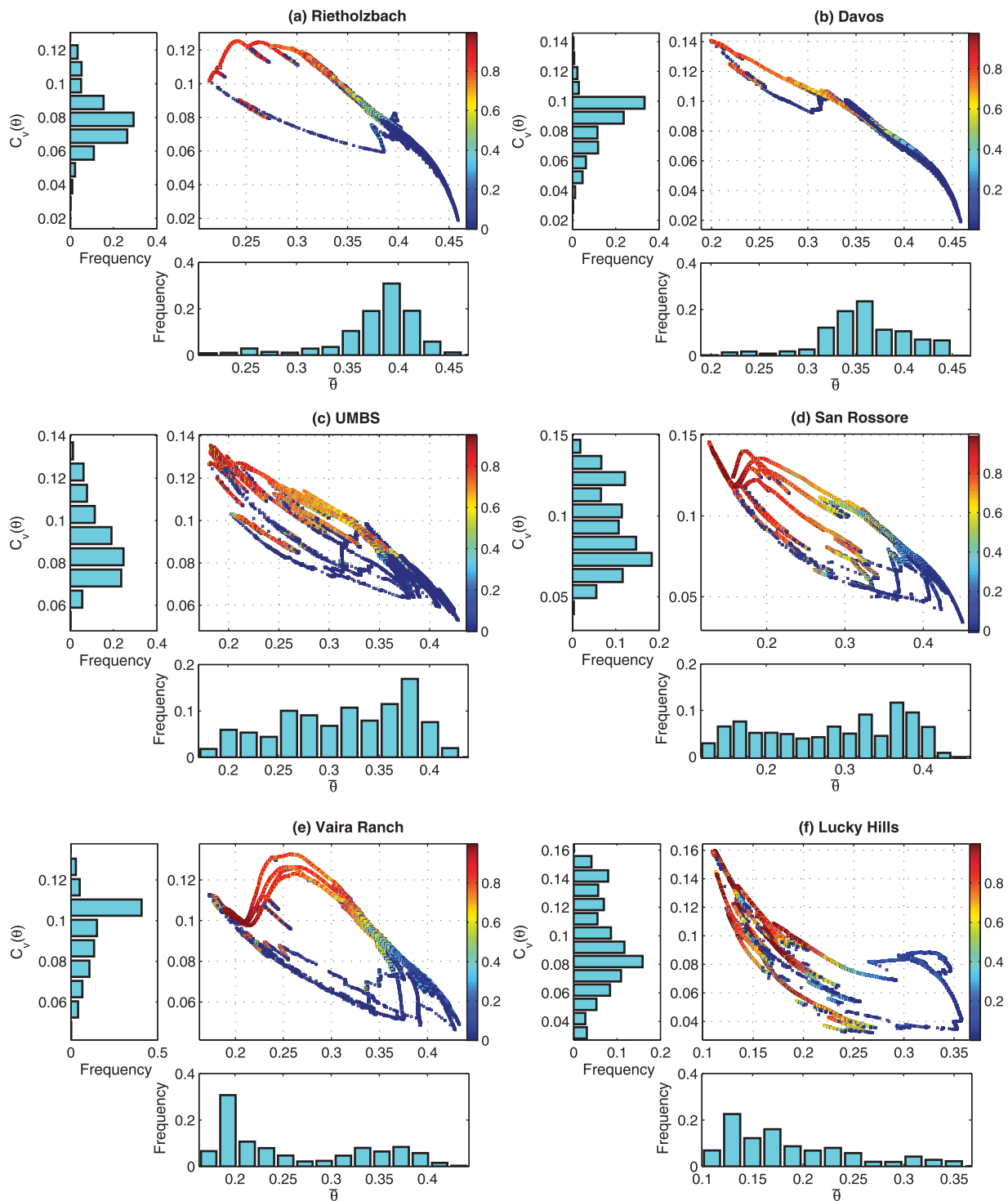


Figure 6. The coefficient of variation of depth-integrated soil moisture content $C_v(\theta)$ as a function of its mean hourly value $\bar{\theta}$ obtained using the **second** soil configuration (heterogenous loam) for the case studies of (a) Rietholzbach, (b) Davos, (c) UMBS, (d) San Rossore, (e) Vaira ranch, and (f) Lucky Hills. The histograms of $C_v(\theta)$ and $\bar{\theta}$ are also illustrated. The color bars indicate for each hour the absolute proportion between biotic controls and abiotic controls scaled between 0 (fully abiotic controlled) and 1 (fully biotic controlled), i.e., $(|T_3|+|T_4|)/(|T_1|+|T_2|+|T_3|+|T_4|)$.

for the Mediterranean locations and UMBS. This decrease is smaller for other two locations, Rietholzbach and Lucky Hills, and almost negligible for Davos, which does not show significant signs of hysteresis even for homogenous soil properties. We visually identify the simulations for the locations of the UMBS and Lucky Hills with the second soil configuration as limiting cases between the occurrence and the lack of

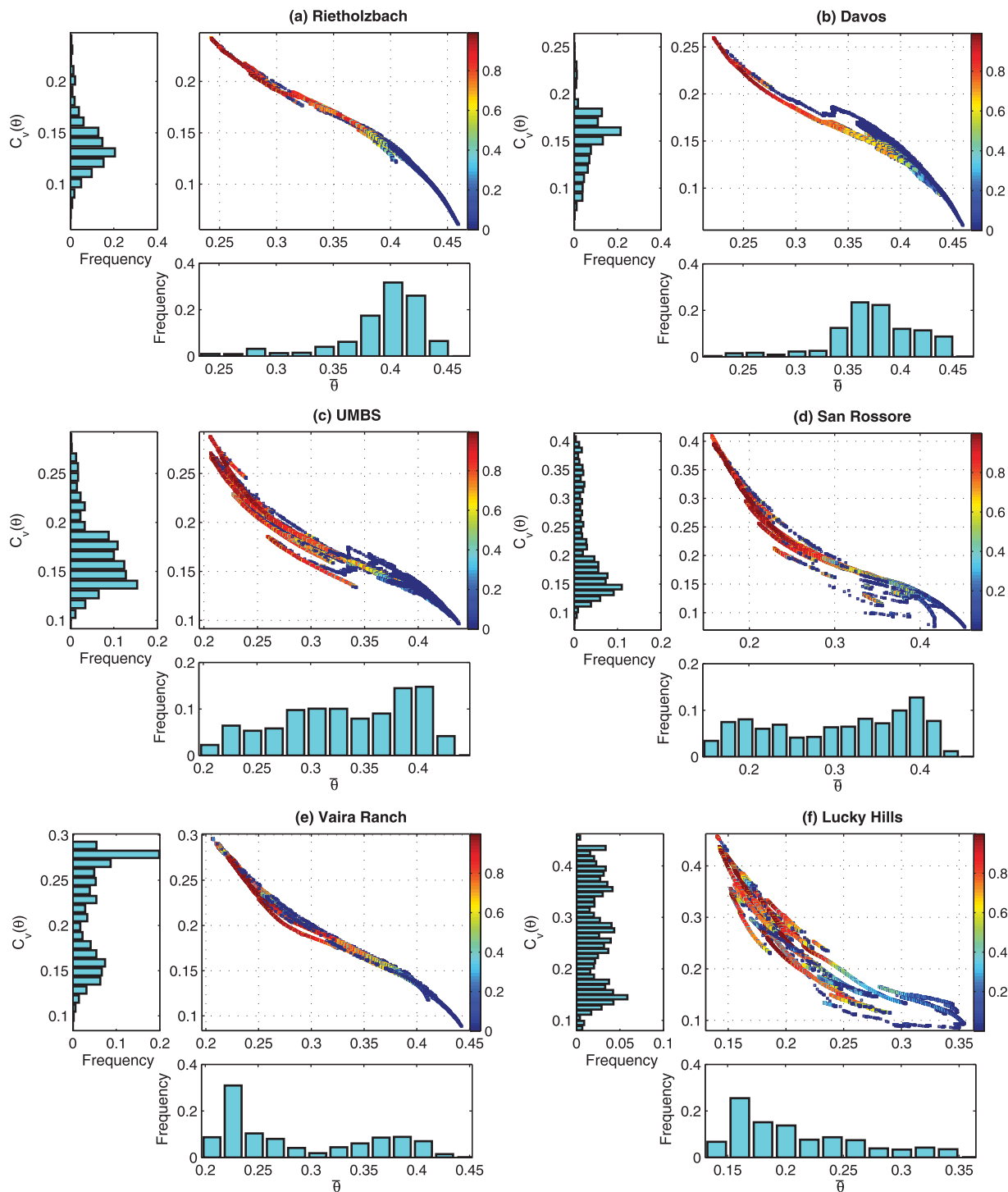


Figure 7. The coefficient of variation of depth-integrated soil moisture content $C_v(\theta)$ as a function of its mean hourly value $\bar{\theta}$ obtained using the **third** soil configuration (fully heterogeneous soil) for the case studies of (a) Rietholzbach, (b) Davos, (c) UMBS, (d) San Rossore, (e) Vaira ranch, and (f) Lucky Hills. The histograms of $C_v(\theta)$ and $\bar{\theta}$ are also illustrated. The color bars indicate for each hour the absolute proportion between biotic controls and abiotic controls scaled between 0 (fully abiotic controlled) and 1 (fully biotic controlled), i.e., $(|T_3|+|T_4|)/(|T_1|+|T_2|+|T_3|+|T_4|)$.

hysteresis (Figure 6). In this way, a numerical threshold for suppression of hysteresis that corresponds to $HY_1 \approx 10$ was identified. Such a threshold is crossed for values of $C_v(K_{sat})$ between 0.16 at Rietholzbach and 0.54 at San Rossore and Vaira ranch (Figure 6) or equivalently for values of the coefficient of variation of residual water content, $C_v(\theta_r)$, between 0.10 and 0.28 (not shown). Even though not easily to

Table 2. Long-Term Simulated Outflow From the Hillslope, Including Surface and Subsurface Runoff, for the Six Locations and the Three Scenarios of Soil Properties, Homogenous, Heterogenous 1, and Heterogenous 2

	Rietholzbach (CH)	Davos (CH)	UMBS (MI)	San Rossore (IT)	Vaira ranch (CA)	Lucky Hills (AZ)
Outflow—Homog. (mm yr ⁻¹)	737	555	168	161	92	25
Outflow—Het. 1 (mm yr ⁻¹)	736	554	169	161	83	26
Outflow—Het. 2 (mm yr ⁻¹)	739	551	166	162	92	52

obtain, $C_v(K_{sat})$ and $C_v(\theta_r)$ are measurable quantities and can assist comparisons between these synthetic results and field observations.

3.4. Comparing Biotic and Abiotic Controls Across Climates

The biotic and abiotic contributions to spatiotemporal variability of soil moisture can be summarized by averaging their relative magnitudes and taking the ratio of these quantities (annual totals), or by computing the relative fractions at the hourly scale and averaging those over the simulation period (hourly fractions) (Figure 9). In both cases, the ratio between biotic ($B=|T_3+T_4|$) and abiotic ($A=|T_1+T_2|$) contributions provides the relative importance of vegetation over physical (climate and soil) controls. Biotic components tend to be larger for both homogenous and heterogenous soils when expressed as hourly fractions rather than annual totals (Figure 9b). This is due to the fact that the magnitude of B can be considerably smaller than A during rainy periods but comparable or larger during the growing season. However, in all of the simulated cases, the ratio B/A is smaller than unity, suggesting a predominance of abiotic factors. Specifically, B/A is about 0.7–1.0 (hourly fractions) or 0.45–0.8 (annual totals) for the locations of Lucky Hills, Vaira ranch and San Rossore, and decreases significantly to 0.1–0.2 for Davos and Rietholzbach. The ratio B/A generally decreases with increasing wetness index, WI (the ratio between precipitation and potential evapotranspiration). The highest values are simulated for seasonal Mediterranean ecosystems (Vaira ranch and San Rossore). Even though semi-arid conditions are represented only with a single location (Lucky Hills, smallest WI in Figure 9), B/A tends to be smaller than for Mediterranean ecosystems, suggesting that the role of vegetation in controlling soil moisture variability is hampered by its sparseness and limited duration of conditions favorable to growth. The inclusion of soil heterogeneity does not affect considerably the overall magnitudes of biotic versus abiotic factors, which tend to be similar for homogenous and heterogeneous

soil properties, especially when annual total contributions are computed (Figure 9a).

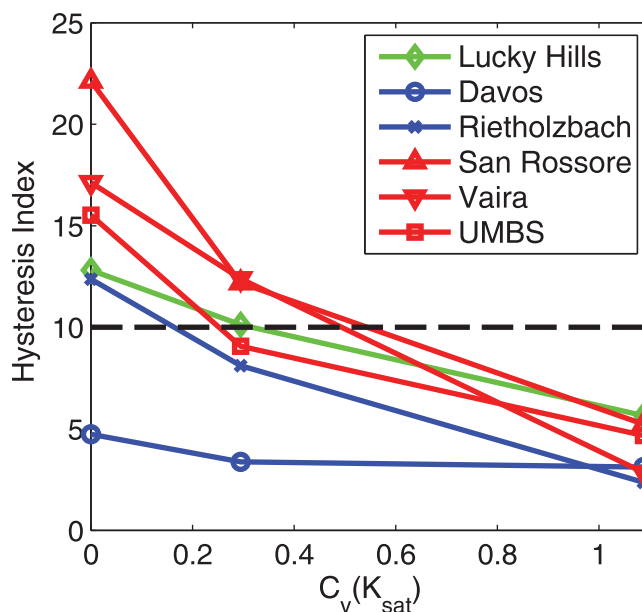


Figure 8. Hysteresis index, HY , defined in equation (14), as a function of the coefficient of variation of the saturated hydraulic conductivity, $C_v(K_{sat})$, for the six analyzed locations. The three $C_v(K_{sat})$ values reflect the three soil heterogeneity levels. The horizontal-dashed line identifies a threshold for the suppression of hysteresis ($HY_r = 10$).

4. Discussion

4.1. Abiotic Versus Biotic Controls

The focus here is on the processes that generate and dissipate heterogeneity in soil moisture at the hillslope scale using a mechanistic ecohydrological model, which simulates hydrological and vegetation dynamics. The model explicitly quantifies the magnitude of the different processes contributing to soil moisture dynamics by solving fluxes and states at the hourly time scale. The quantification of these contributions is far from being obvious and was only possible through a mechanistic ecohydrological model in

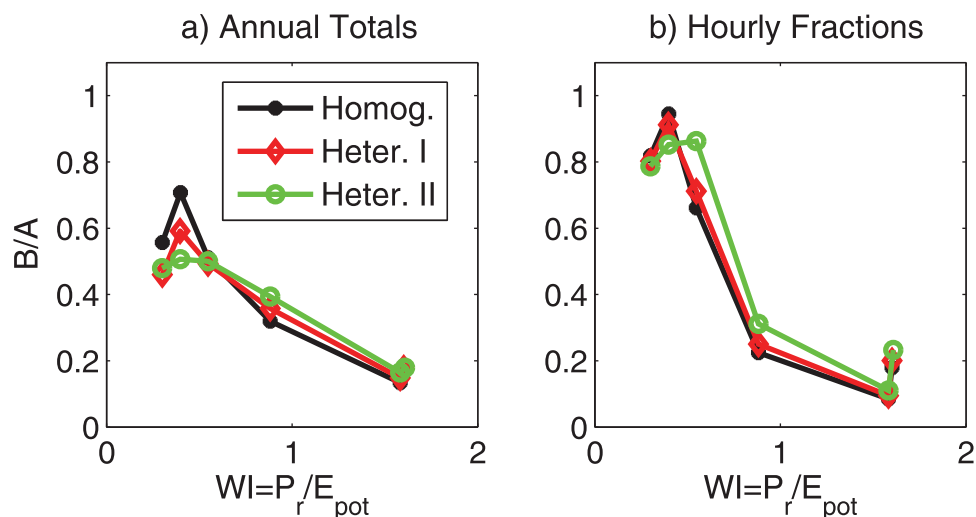


Figure 9. The average ratio between the biotic ($B=|T_3+T_4|$) and the abiotic ($A=|T_1+T_2|$) components computed as annual totals (a) and hourly fractions (b), as a function of the Wetness Index (WI), i.e., precipitation divided by potential evapotranspiration for the three soil configurations: homogenous loam (Homog.), heterogenous loam (Heter. I), and fully heterogenous soil (Heter. II). Potential evapotranspiration over the hillslope was computed from simulated net radiation.

combination with the analytical derivation of equation (13). Thus, one of the main novelties here is an explicit quantification of the role of abiotic versus biotic controls on depth-integrated soil moisture spatiotemporal variability at the hillslope scale.

The study complements and expands the previous approaches that were limited by (i) the purely theoretical framework [Albertson and Montaldo, 2003], (ii) the level of detail of the analyzed processes [Teuling and Troch, 2005; Teuling et al., 2007a], (iii) the spatial dimension [Katul et al., 1997], and (iv) the specificity of the location [Ivanov et al., 2010; Rosenbaum et al., 2012; Sela et al., 2012]. Four terms, T_1 , T_2 , T_3 , and T_4 , were derived (equation (13)) to separate biotic from abiotic contributions to changes in soil moisture spatial variance and mean. The most significant effects are produced by precipitation and lateral redistribution (abiotic), and transpiration (biotic). Precipitation decreases variability (negative T_2) in wet to mildly wet conditions and increases variability (positive T_2) for dry conditions, while lateral redistribution acts as a factor that enhances spatial variability of soil moisture (positive T_2). Vegetation has a dual effect: through transpiration it can both increase and decrease the soil moisture variance (positive and negative T_4 , respectively). Its role depends on soil moisture distribution in the domain but mostly on its mean ($\bar{\theta}$). The term T_4 is positive for relatively high soil moisture contents, due to variability in the incoming energy and canopy biophysical properties (e.g., LAI), and becomes negative when the hillslope dries and vegetation experiences water stress. In this situation, larger transpiration rates from wetter areas tend to homogenize the system. The switch in the vegetation role is clearly visible for the homogenous soil conditions and it occurs after $C_v(\bar{\theta})$ has reached its maximum value (Figure 5). The corresponding $\bar{\theta}$ represents the value where vegetation in the hillslope starts to be water limited.

The biotic controls on $\frac{\partial C_v}{\partial t}$ were found to be around 10–30% of the abiotic ones for the Swiss locations with large wetness indexes (the ratio between annual precipitation and potential evapotranspiration). Their importance increased up to 50–60% computed as annual totals (or 80–90% computed as hourly fractions) at the drier end of the examined locations (San Rossore, Vaira ranch, and Lucky Hills). The importance of biotic controls peaks for intermediate values of the wetness index (around 0.4). The aforementioned wetness index coincides with the Mediterranean climates where growing seasons are out of phase with precipitation, leading to a distinct dry season where vegetation exerts a dominant role. While the results are limited by the analysis of a single typical location in a semi-arid climate (Lucky Hills), they appear to indicate that vegetation importance on C_v decreases for very dry and wet conditions. In essence, climate through precipitation, evapotranspiration, and seasonality determines the type of vegetation and the relative importance of biotic and abiotic controls.

4.2. Hysteresis of the $C_v(\theta)$ - $\bar{\theta}$ Relation and Link with Field Observations

A comparison of the $C_v(\theta)$ - $\bar{\theta}$ diagrams for different climate and vegetation types and heterogeneity in soil properties offers plausible explanations as to why hysteresis in the $C_v(\theta)$ - $\bar{\theta}$ relation is rarely seen in observations, while decreasing exponential or linear functions typically describe well empirical data [Penna *et al.*, 2009; Brocca *et al.*, 2010; Tague *et al.*, 2010; Brocca *et al.*, 2012]. First of all, we consider moisture dynamics attributed to the entire soil thickness, which includes both vadose zone and phreatic aquifer. Considering only a surficial layer, as is the case in many empirical studies due to constraints of instrumenting deep soil locations can overemphasize the vadose zone dynamics in progressively drier climates. This is due to the “uncoupling” of near-surface moisture content dynamics and lateral water exchanges in the saturated soil above the bedrock. Secondly, observations are unlikely to span the full range of $\bar{\theta}$ [but see Rosenbaum *et al.*, 2012, for a notable exception] because sporadic distributed measurements of soil moisture are particularly challenging in very dry conditions due to soil hardness [e.g., Brocca *et al.*, 2012]; very wet conditions that occur during or immediately after significant precipitation events are also rarely monitored. Additionally, heterogeneity of soil properties and other localized hillslope characteristics that are not considered in our analysis (e.g., variability in rock content, microtopography, differences in canopy and subcanopy structure, and difference in the litter layer) are likely to play out in the same direction, reducing or eliminating hysteresis altogether and favoring a negative relation between $C_v(\theta)$ and $\bar{\theta}$. Note that published values of $C_v(\theta)$ [e.g., Brocca *et al.*, 2007; Famiglietti *et al.*, 2008; Brocca *et al.*, 2010; Tague *et al.*, 2010] are closer to the values simulated here for fully heterogeneous soil, rather than for the other soil configurations, thereby reinforcing the above argument. We also quantify how much soil heterogeneity, expressed using $C_v(K_{sat})$ or $C_v(\theta_r)$, is needed to suppress hysteresis ($HY_l < 10$). When $C_v(K_{sat})$ exceeds ≈ 0.15 for wet climates and ≈ 0.55 for Mediterranean climates, hysteresis becomes very unlikely (Figure 6) and the $C_v(\theta)$ - $\bar{\theta}$ relation tends to become unique. Note that $C_v(K_{sat})$ larger than 0.2–0.6 (or equivalently standard deviations of $\ln(K_{sat}) \approx 0.2$ –1.0) are far from being unrealistic in field observations [e.g., Cosby *et al.*, 1984; Elsenbeer *et al.*, 1992; Mallants *et al.*, 1997]. Lastly, sampling volume of conventional soil moisture sensors is quite small (few dozens of cm^3), as compared to the Representative Elementary Volumes of effective soil hydraulic properties. This implies that soil moisture observation is subject to local (measurement scale) noise that is superimposed on variations of properties at the hillslope scale, further impacting interpretations of $C_v(\theta)$ - $\bar{\theta}$ relations.

The observational result that a normal distribution is typically a “good fit” for the temporal variability of the spatial mean of soil moisture $\bar{\theta}$ [e.g., Vachaud *et al.*, 1985; Anctil *et al.*, 2002; Brocca *et al.*, 2007] can be also ascribed to the limitations in the range and depth of typically measured distributed soil water contents, as supported by more complex distributions identified in the numerical analysis for all of the soil configurations here (Figure 5 and 7).

Hence, it may be conjectured that in the presence of heterogeneous soil properties or other types of local heterogeneities, the observed $C_v(\theta)$ is mostly reflecting signatures of these variations rather than the effects of climate, vegetation, or topography as also discussed by other authors [Choi *et al.*, 2007; Martínez García *et al.*, 2014]. This consideration may explain why it has been difficult to detect clear biotic and abiotic controls on soil moisture variability from observations only. Undoubtedly, exceptions exist as may be the case for the homogenous sandy soils (e.g., at the UMBS or in the Kalahari region [Scanlon *et al.*, 2007; He *et al.*, 2013]), but we argue that a similar inference would be even more relevant at spatial scales larger than the B2 hillslope, where soil heterogeneities are likely to be more pronounced. The imposed heterogeneity in the third soil configuration was exaggerated precisely to clarify this aspect. Such a finding has implications on the design of observational soil moisture network. Filtering out soil heterogeneities, for instance using soil water potential, a transformation of the statistical distribution of θ , or looking at temporal anomalies [Mittelbach and Seneviratne, 2012; Brocca *et al.*, 2014], would be necessary if the interest lays on identifying climate, vegetation, and topographic controls on soil moisture spatiotemporal variability.

4.3. Limits of Interpretation

Despite attempts to generalize findings across different locations, this study has limitations, the major one being the single domain of a fairly small size (15 m \times 30 m). While the B2 hillslope can be regarded as a representative hillslope, additional analyses with domains differing in topography and size (from headwater catchments to mesoscale catchments) represent a logical extension. The use of a larger domain will also allow for a more realistic representation of spatial correlation and variability of soil properties [e.g., Western

et al., 2004]. Vegetation cover is also assumed to be uniform within the domain, which may be not necessarily the case. The assumption of uniform 1 m soil depth was not found to be crucial as similar findings were obtained with a soil depth of 0.6 m and 3.0 m (not shown). Replacing an impermeable bottom with a free drainage condition however canceled the effect of the three-dimensional domain (not shown), because the hillslope dynamics become almost one-dimensional and spatial heterogeneity is strongly suppressed ($C_v(\theta)$ is almost constant) in all of the climates and analyzed configurations.

An additional limitation is related to the representation of vegetation functioning and specifically for this study of the water uptake component. T&C, similar to other vegetation and ecohydrological models, has a simplified representation of several plant components dictated by modeling assumptions and limited knowledge of physiological and ecological processes [e.g., Pappas *et al.*, 2013]. Certain processes are not even included as the temporal variability of rooting depth, hydraulic redistribution through roots, seasonality and acclimation of photosynthetic properties, direct environmental controls on plant growth. However, for the objectives of this study, we argue that T&C provides an accurate approximation of vegetation functioning and soil moisture spatiotemporal variability.

5. Conclusions

An analytical expression to separate the role of different terms in the temporal dynamics of soil moisture spatial variability (equation (13)) was combined with the numerical results of a mechanistic ecohydrological model, T&C. The model allowed continuous simulations of soil moisture spatiotemporal dynamics ($\bar{\theta}$ and $C_v(\theta)$) at an exemplary hillslope domain, for six case studies differing in climate and vegetation, and for three different configurations of soil properties. Using this framework, we explicitly quantified the importance of biotic and abiotic controls on spatiotemporal soil moisture variability.

In the examined case studies, abiotic (A) controls are always larger than biotic (B) ones ($B/A < 1$) and are dominant in wet climates where $B/A \approx 0.1-0.2$. The maximum of B/A is obtained for Mediterranean climates ($B/A=0.7-1.0$) and is favored by having the seasonality of vegetation and climate that is out of phase. The ratio B/A decreases again for the analyzed semiarid location, suggesting that the biotic controls may become smaller at the dry end of the climate spectrum.

The relation between the spatial coefficient of variation and mean soil moisture $C_v(\theta) - \bar{\theta}$ was found to be unique and well described by an exponential or linear function for the Swiss locations (Rietholzbach and Davos), regardless of the soil properties. Strong hysteretic cycles were observed for the Mediterranean locations (Vaira ranch and San Rossore) and, to a lesser extent, at the UMBS for homogenous soil textural properties. Lucky Hills was mostly characterized by dry conditions and low spatial variability. Heterogeneity in soil properties increases $C_v(\theta)$ to magnitudes commensurable with field observations and tends to mask hysteresis in all of the locations. While soil heterogeneity was intentionally exaggerated in these numerical simulations, given the size of the hillslope, it served the purpose of highlighting this fundamental aspect. Heterogeneity in soil (but other local heterogeneities in canopy gaps, litter layer, microtopography are argued to contribute in the same direction) can obscure or hide climatic and biotic controls of soil moisture spatiotemporal variability. They likely explain why common field observations report a unique relation and a strong negative correlation between $C_v(\theta)$ and $\bar{\theta}$.

References

- Albertson, J. D., and N. Montaldo (2003), Temporal dynamics of soil moisture variability. 1. Theoretical basis, *Water Resour. Res.*, *39*(10), 1274, doi:10.1029/2002WR001616.
- Ancil, F., R. Mathieu, L. E. Parent, A. A. Viau, M. Sbih, and M. Hessami (2002), Geostatistics of near-surface moisture in bare cultivated organic soils, *J. Hydrol.*, *260*, 30–37.
- Arora, V. K., and G. J. Boer (2005), A parameterization of leaf phenology for the terrestrial ecosystem component of climate models, *Global Change Biol.*, *11*(1), 39–59.
- Assouline, S., and Y. Mualem (2006), Runoff from heterogeneous small bare catchments during soil surface sealing, *Water Resour. Res.*, *42*, W12405, doi:10.1029/2005WR004592.
- Baldocchi, D. D., L. Xu, and N. Kiang (2004), How plant functional-type, weather, seasonal drought, and soil physical properties alter water and energy fluxes of an oak-grass savanna and an annual grassland, *Agric. For. Meteorol.*, *123*, 13–39, doi:10.1016/j.agrformet.2003.11.006.
- Bonan, G. B., P. J. Lawrence, K. W. Oleson, S. Levis, M. Jung, M. Reichstein, D. M. Lawrence, and S. C. Swenson (2011), Improving canopy processes in the Community Land Model version 4 (CLM4) using global flux fields empirically inferred from FLUXNET data, *J. Geophys. Res.*, *116*, G02014, doi:10.1029/2010JG001593.

Acknowledgments

G.G.K. acknowledges the support from the National Science Foundation (AGS-1102227, NSF-EAR 1344703), the U.S. Department of Agriculture (2011–67003-30222), the Binational Agricultural Research and Development (BARD) Fund (IS-4374-11C), and the U.S. Department of Energy through the Office of Biological and Environmental Research (BER) Terrestrial Carbon Processes (TCP) program (DE-SC000697 and DE-SC0011461). V.I. was partially supported by the NSF Grant EAR 1151443 and the Visiting Faculty Grant at the Institute of Environmental Engineering, ETH Zürich. A.P. acknowledges the financial support of the Swiss National Science Foundation and the Stavros Niarchos Foundation through the SNSF Early Postdoc Mobility Fellowship (P2EZP2–152244). All of the simulation results are freely available upon request to the corresponding author.

- Brocca, L., F. Melone, T. Moramarco, and R. Morbidelli (2010), Spatial-temporal variability of soil moisture and its estimation across scales, *Water Resour. Res.*, *46*, W02516, doi:10.1029/2009WR008016.
- Brocca, L., R. Morbidelli, F. Melone, and T. Moramarco (2007), Soil moisture spatial variability in experimental areas of central Italy, *J. Hydrol.*, *333*, 356–373.
- Brocca, L., T. Tullio, F. Melone, T. Moramarco, and R. Morbidelli (2012), Catchment scale soil moisture spatial-temporal variability, *J. Hydrol.*, *422–423*, 63–75.
- Brocca, L., G. Zucco, H. Mittelbach, T. Moramarco, and S. I. Seneviratne (2014), Absolute versus temporal anomaly and percent of saturation soil moisture spatial variability for six networks worldwide, *Water Resour. Res.*, *50*, 5560–5576, doi:10.1002/2014WR015684.
- Chiesi, M., F. Maselli, M. Moriondo, L. Fibbi, M. Bindi, and S. Running (2007), Application of BIOME-BGC to simulate Mediterranean forest processes, *Ecol. Modell.*, *206*, 179–190, doi:10.1016/j.ecolmodel.2007.03.032.
- Choi, M., and J. M. Jacobs (2007), Soil moisture variability of root zone profiles within SMEX02 remote sensing footprints, *Adv. Water Res.*, *30*, 883–896.
- Choi, M., J. M. Jacobs, and M. H. Cosh (2007), Scaled spatial variability of soil moisture fields, *Geophys. Res. Lett.*, *34*, L01401, doi:10.1029/2006GL028247.
- Churakova (Sidorova), O. V., W. Eugster, S. Etzold, P. Cherubini, S. Zielis, M. Saurer, R. Siegwolf, and N. Buchmann (2014), Increasing relevance of spring temperatures for Norway spruce trees in Davos, Switzerland, after the 1950s, *Trees*, *28*, 183–191.
- Cosby, B. J., G. M. Hornberger, R. B. Clapp, and T. R. Ginn (1984), A statistical exploration of the relationships of soil moisture characteristics to the physical properties of soils, *Water Resour. Res.*, *20*(6), 682–690.
- Cosh, M., T. Jackson, S. Moran, and R. Bindlish (2008), Temporal persistence and stability of surface soil moisture in a semi-arid watershed, *Remote Sens. Environ.*, *112*(2), 304–313.
- Crow, W. T., D. Ryu, and J. S. Famiglietti (2005), Upscaling of field-scale soil moisture measurements using distributed land surface modeling, *Adv. i Water Resour.*, *28*, 1–14.
- Curtis, P. S., C. S. Vogel, C. M. Gough, H. P. Schmid, H. B. Su, and B. D. Bovard (2005), Respiratory carbon losses and the carbon-use efficiency of a northern hardwood forest, 1999–2003, *New Phytol.*, *167*(2), 437–455.
- Dirmeyer, P. A., R. D. Koster, and Z. Guo (2006), Do global models properly represent the feedback between land and atmosphere?, *J. Hydrometeorol.*, *7*, 1177–1198.
- Dorigo, W. A., et al. (2011), The International Soil Moisture Network: A data hosting facility for global in situ soil moisture measurements, *Hydrol. Earth Syst. Sci.*, *15*(5), 1675–1698.
- Dorigo, W. A., A. Xavier, M. Vreugdenhil, A. Gruber, A. Hegyiová, A. D. Sanchis-Dufau, D. Zamojski, C. Cordes, W. Wagner, and M. Drusch (2013), Global automated quality control of in situ soil moisture data from the International Soil Moisture Network, *Vadose Zone J.*, *12*(3), doi:10.2136/vzj2012.0097.
- Elsenbeer, H., K. Cassel, and J. Castro (1992), Spatial analysis of soil hydraulic conductivity in a tropical rain forest catchment, *Water Resour. Res.*, *28*(12), 3201–3214.
- Emmerich, W. E., and C. L. Verdugo (2008), Long-term carbon dioxide and water flux database, Walnut Gulch Experimental Watershed, Arizona, United States, *Water Resour. Res.*, *44*, W05509, doi:10.1029/2006WR005693.
- Etzold, S., N. K. Ruehr, R. Zweifel, M. Dobbertin, A. Zingg, P. Pluess, R. Häslar, W. Eugster, and N. Buchmann (2011), The carbon balance of two contrasting mountain forest ecosystems in Switzerland: Similar annual trends, but seasonal differences, *Ecosystems*, *14*(8), 1289–1309, doi:10.1007/s10021-011-9481-3.
- Famiglietti, J. S., J. A. Devereaux, C. Laymon, T. Tsegaye, P. R. Houser, T. J. Jackson, S. T. Graham, M. Rodell, and P. J. van Oevelen (1999), Ground-based investigation of spatial-temporal soil moisture variability within remote sensing footprints during Southern Great Plains 1997 (SGP97) Hydrology Experiment, *Water Resour. Res.*, *35*(6), 1839–1851.
- Famiglietti, J. S., D. Ryu, A. A. Berg, M. Rodell, and T. J. Jackson (2008), Field observations of soil moisture variability across scales, *Water Resour. Res.*, *44*, W01423, doi:10.1029/2006WR005804.
- Farquhar, G. D., S. V. Caemmerer, and J. A. Berry (1980), A biochemical model of photosynthetic CO₂ assimilation in leaves of C₃ species, *Planta*, *149*, 78–90.
- Fatichi, S. (2010), The modeling of hydrological cycle and its interaction with vegetation in the framework of climate change, PhD thesis, Univ. of Firenze, Italy.
- Fatichi, S., and V. Y. Ivanov (2014), Interannual variability of evapotranspiration and vegetation productivity, *Water Resour. Res.*, *50*, 3275–3294, doi:10.1002/2013WR015044.
- Fatichi, S., and S. Leuzinger (2013), Reconciling observations with modeling: The fate of water and carbon allocation in a mature deciduous forest exposed to elevated CO₂, *Agric. For. Meteorol.*, *174–175*, 144–157, doi:10.1016/j.agrformet.2013.02.005.
- Fatichi, S., V. Y. Ivanov, and E. Caporali (2012a), A mechanistic ecohydrological model to investigate complex interactions in cold and warm water-controlled environments. 1 Theoretical framework and plot-scale analysis, *J. Adv. Model. Earth Syst.*, *4*, M05002, doi:10.1029/2011MS000086.
- Fatichi, S., V. Y. Ivanov, and E. Caporali (2012b), A mechanistic ecohydrological model to investigate complex interactions in cold and warm water-controlled environments. 2 Spatiotemporal analyses, *J. Adv. Model. Earth Syst.*, *4*, M05003, doi:10.1029/2011MS000087.
- Fatichi, S., M. J. Zeeman, J. Fuhrer, and P. Burlando (2014), Ecohydrological effects of management on subalpine grasslands: From local to catchment scale, *Water Resour. Res.*, *50*, 148–164, doi:10.1002/2013WR014535.
- Gaur, N., and B. P. Mohanty (2013), Evolution of physical controls for soil moisture in humid and subhumid watersheds, *Water Resour. Res.*, *49*, 1244–1258, doi:10.1002/wrcr.20069.
- Gough, C. M., C. E. Flower, C. S. Vogel, D. Dragoni, and P. S. Curtis (2009), Whole-ecosystem labile carbon production in a north temperate deciduous forest, *Agric. For. Meteorol.*, *149*, 1531–1540, doi:10.1016/j.agrformet.2009.04.006.
- Gough, C. M., B. S. Hardiman, L. E. Nave, G. Bohrer, K. D. Maurer, C. S. Vogel, K. J. Nadelhoffer, and P. S. Curtis (2013), Sustained carbon uptake and storage following moderate disturbance in a great lakes forest, *Ecol. Appl.*, *23*(5), 1202–1215.
- Granier, A., et al. (2007), Evidence for soil water control on carbon and water dynamics in European forests during the extremely dry year: 2003, *Agric. For. Meteorol.*, *143*, 123–145.
- Grayson, R. B., and A. W. Western (1998), Towards areal estimation of soil water content from point measurements: Time and space stability of mean response, *J. Hydrol.*, *207*, 68–82, doi:10.1016/S0022-1694(98)00096-1.
- Grayson, R. B., A. W. Western, F. H. S. Chiew, and G. Blöschl (1997), Preferred states in spatial soil moisture patterns: Local and nonlocal controls, *Water Resour. Res.*, *33*(12), 2897–2908.
- Gruber, A., W. A. Dorigo, S. Zwieback, A. Xavier, and W. Wagner (2013), Characterizing coarse-scale representativeness of in-situ soil moisture measurements from the International Soil Moisture Network, *Vadose Zone J.*, *12*(2), doi:10.2136/vzj2012.0170.

- He, L., V. Y. Ivanov, G. Bohrer, J. E. Thomsen, C. S. Vogel, and M. Moghaddam (2013), Temporal dynamics of soil moisture in a northern temperate mixed successional forest after a prescribed intermediate disturbance, *Agric. For. Meteorol.*, *180*, 22–33, doi:10.1016/j.agrformet.2013.04.014.
- He, L., V. Y. Ivanov, G. Bohrer, K. D. Maurer, C. S. Vogel, and M. Moghaddam (2014), Effects of fine-scale soil moisture and canopy heterogeneity on energy and water fluxes in a northern temperate mixed forest, *Agric. For. Meteorol.*, *184*, 243–256, doi:10.1016/j.agrformet.2013.10.006.
- Hopp, L., C. Harman, S. Desilets, C. Graham, J. McDonnell, and P. A. Troch (2009), Hillslope hydrology under glass: Confronting fundamental questions of soil-water-biota co-evolution at Biosphere 2, *Hydrol. Earth Syst. Sci.*, *13*(11), 2105–2118.
- Hu, W., M. Shao, F. Han, K. Reichardt, and J. Tan (2010), Watershed scale temporal stability of soil water content, *Geoderma*, *158*, 181–198.
- Huxman, T., P. Troch, J. Chorover, D. D. Breshears, S. Saleska, X. Z. J. Pelletier, and J. Espeleta (2009), The hills are alive: Earth science in a controlled environment, *Eos Trans. AGU*, *34*(90), 120.
- Ivanov, V. Y., E. R. Vivoni, R. L. Bras, and D. Entekhabi (2004), Preserving high-resolution surface and rainfall data in operational-scale basin hydrology: A fully-distributed physically-based approach, *J. Hydrol.*, *298*, 80–111, doi:10.1016/j.jhydrol.2004.03.041.
- Ivanov, V. Y., R. L. Bras, and E. R. Vivoni (2008), Vegetation-hydrology dynamics in complex terrain of semiarid areas. 1. A mechanistic approach to modeling dynamic feedbacks, *Water Resour. Res.*, *44*, W03429, doi:10.1029/2006WR005588.
- Ivanov, V. Y., S. Fatichi, G. D. Jenerette, J. F. Espeleta, P. A. Troch, and T. E. Huxman (2010), Hysteresis of soil moisture spatial heterogeneity and the homogenizing effect of vegetation, *Water Resour. Res.*, *46*, W09521, doi:10.1029/2009WR008611.
- Jacobs, J. M., B. P. Mohanty, H. En-Ching, and D. Miller (2008), SMEX02: Field scale variability, time stability and similarity of soil moisture, *Remote Sens. Environ.*, *92*, 436–446, doi:10.1016/j.rse.2004.02.017.
- Juang, J.-Y., G. G. Katul, A. Porporato, P. C. Stoy, M. S. Siqueira, M. Detto, H.-S. Kim, and R. Oren (2007), Eco-hydrological controls on summer-time convective rainfall triggers, *Global Change Biol.*, *13*, 887–896, doi:10.1111/j.1365-2486.2006.01315.x.
- Katul, G. G., P. Todd, D. Pataki, Z. J. Kabala, and R. Oren (1997), Soil water depletion by oak trees and the influence of root water uptake on moisture content spatial statistics, *Water Resour. Res.*, *33*(4), 611–623, doi:10.1029/96WR03978.
- Katul, G. G., A. Porporato, E. Daly, A. C. Oishi, H.-S. Kim, P. C. Stoy, J.-Y. Juang, and M. B. Siqueira (2007), On the spectrum of soil moisture from hourly to interannual scales, *Water Resour. Res.*, *43*, W05428, doi:10.1029/2006WR005356.
- Keefer, T. O., M. S. Moran, and G. B. Paige (2008), Long-term meteorological and soil hydrology database, Walnut Gulch Experimental Watershed, Arizona, United States, *Water Resour. Res.*, *44*, W05S07, doi:10.1029/2006WR005702.
- Kim, J., and V. Y. Ivanov (2014), On the nonuniqueness of sediment yield at the catchment scale: The effects of soil antecedent conditions and surface shield, *Water Resour. Res.*, *50*, 1025–1045, doi:10.1002/2013WR014580.
- Lawrence, J. E., and G. M. Hornberger (2007), Soil moisture variability across climate zones, *Geophys. Res. Lett.*, *34*, L20402, doi:10.1029/2007GL031382.
- Legates, D. R., R. Mahmood, D. F. Levita, T. L. DeLiberty, S. M. Quiring, C. Houser, and F. E. Nelson (2011), Soil moisture: A central and unifying theme in physical geography, *Prog. Phys. Geogr.*, *35*(1), 65–86.
- Leuzinger, S., G. Zott, R. Asshoff, and C. Körner (2005), Responses of deciduous forest trees to severe drought in Central Europe, *Tree Physiol.*, *25*, 641–650.
- Ma, S., D. D. Baldocchi, L. Xu, and T. Hehn (2007), Inter-annual variability in carbon dioxide exchange of an oak/grass savanna and open grassland in California, *Agric. For. Meteorol.*, *147*, 157–171, doi:10.1016/j.agrformet.2007.07.008.
- Mallants, D., B. P. Mohanty, A. Vervoort, and J. Feyen (1997), Spatial analysis of saturated hydraulic conductivity in a soil with macropores, *Soil Technol.*, *10*, 115–131.
- Martínez García, G., Y. A. Pachepsky, and H. Vereecken (2014), Effect of soil hydraulic properties on the relationship between the spatial mean and variability of soil moisture, *J. Hydrol.*, *516*, 154–160.
- Martínez, G., Y. A. Pachepsky, H. Vereecken, H. Hardelauf, M. Herbst, and K. Vanderlinden (2013), Modeling local control effects on the temporal stability of soil water content, *J. Hydrol.*, *481*, 106–118.
- Mellor, G. L., and T. Yamada (1982), Development of a turbulence closure model for geophysical fluid problems, *Rev. Geophys.*, *20*(4), 871–875, doi:10.1029/RG020i004p00851.
- Mittelbach, H., and S. I. Seneviratne (2012), A new perspective on the spatio-temporal variability of soil moisture: Temporal dynamics versus time invariant contributions, *Hydrol. Earth Syst. Sci.*, *16*, 2169–2179.
- Montaldo, N., and J. D. Albertson (2003), Temporal dynamics of soil moisture variability. 2. implications for land surface models, *Water Resour. Res.*, *39*(10), 1275, doi:10.1029/2002WR001618.
- Pappas, C., S. Fatichi, S. Leuzinger, A. Wolf, and P. Burlando (2013), Sensitivity analysis of a process-based ecosystem model: pinpointing parameterization and structural issues, *J. Geophys. Res. – Biogeosciences*, *118*(2), 505–528, doi:10.1002/jgrg.20035.
- Pappas, C., S. Fatichi, S. Rimkus, P. Burlando, and M. O. Huber, (2015), The role of local scale heterogeneities in terrestrial ecosystem modeling, *J. Geophys. Res. – Biogeosciences*, *120*(2), 341–360, doi:10.1002/2014JG002735.
- Penna, D., M. Borga, D. Norbiato, and G. Dalla Fontana (2009), Hillslope scale soil moisture variability in a steep alpine terrain, *J. Hydrol.*, *364*(3–4), 311–327, doi:10.1016/j.jhydrol.2008.11.009.
- Porporato, A., F. Laio, L. Ridolfi, and I. Rodriguez-Iturbe (2001), Plants in water-controlled ecosystems: Active role in hydrologic processes and response to water stress. III. Vegetation water stress, *Adv. Water Resour.*, *24*, 725–744.
- Robinson, D. A., C. S. Campbell, J. W. Hopmans, B. K. Hornbuckle, S. B. Jones, R. Knight, F. Ogden, J. Selker, and O. Wendroth (2008), Soil moisture measurements for ecological and hydrological watershed scale observatories: A review, *Vadose Zone J.*, *7*, 358–389, doi:10.2136/vzj2007.0143.
- Rosenbaum, U., H. R. Bogen, M. Herbst, J. A. Huisman, T. J. Peterson, A. Weuthen, A. W. Western, and H. Vereecken (2012), Seasonal and event dynamics of spatial soil moisture patterns at the small catchment scale, *Water Resour. Res.*, *48*, W10544, doi:10.1029/2011WR011518.
- Ryu, Y., D. D. Baldocchi, S. Ma, and T. Hehn (2008), Interannual variability of evapotranspiration and energy exchange over an annual grassland in California, *J. Geophys. Res.*, *113*, D09104, doi:10.1029/2007JD009263.
- Saghafian, B., P. Julien, and F. Ogden (1995), Similarity in catchment response 1. Stationary rainstorms, *Water Resour. Res.*, *31*(6), 1533–1541, doi:10.1029/95WR00518.
- Saxton, K. E., and W. J. Rawls (2006), Soil water characteristic estimates by texture and organic matter for hydrologic solutions, *Soil Sci. Soc. Am. J.*, *70*, 1569–1578, doi:10.2136/sssaj2005.0117.
- Scanlon, T. M., K. K. Caylor, S. A. Levin, and I. Rodriguez-Iturbe (2007), Positive feedbacks promote power-law clustering of Kalahari vegetation, *Nature*, *449*, 209–212, doi:10.1038/nature06060.

- Sela, S., T. Svoray, and S. Assouline (2012), Soil water content variability at the hillslope scale: Impact of surface sealing, *Water Resour. Res.*, *48*, W03522, doi:10.1029/2011WR011297.
- Seneviratne, S. I., D. Lüthi, M. Litschi, and C. Schär (2006), Land-atmosphere coupling and climate change in Europe, *Nature*, *443*, 205–209.
- Seneviratne, S. I., T. Corti, E. L. Davin, M. Hirschi, E. B. Jaeger, I. Lehner, B. Orlowsky, and A. J. Teuling (2010), Investigating soil moisture–climate interactions in a changing climate: A review, *Earth Sci. Rev.*, *99*(3–4), 125–161.
- Seneviratne, S. I., et al. (2012), Swiss prealpine Rietholz bach research catchment and lysimeter: 32 year time series and 2003 drought event, *Water Resour. Res.*, *48*, W06526, doi:10.1029/2011WR011749.
- Tague, C., L. Band, S. Kenworthy, and D. Tenebaum (2010), Plot- and watershed-scale soil moisture variability in a humid piedmont watershed, *Water Resour. Res.*, *46*, W12541, doi:10.1029/2009WR008078.
- Teuling, A. J., and P. A. Troch (2005), Improved understanding of soil moisture variability dynamics, *Geophys. Res. Lett.*, *32*, L05404, doi:10.1029/2004GL021935.
- Teuling, A. J., F. Hupet, R. Uijlenhoet, and P. A. Troch (2007a), Climate variability effects on spatial soil moisture dynamics, *Geophys. Res. Lett.*, *34*, L06406, doi:10.1029/2006GL029080.
- Teuling, A. J., R. Uijlenhoet, R. Hurkmans, O. Merlin, R. Panciera, J. P. Walker, and P. A. Troch (2007b), Dry-end surface soil moisture variability during NAFE'06, *Geophys. Res. Lett.*, *34*, L17402, doi:10.1029/2007GL031001.
- Teuling, A. J., I. Lehner, J. W. Kirchner, and S. I. Seneviratne (2010), Catchments as simple dynamical systems: Experience from a Swiss prealpine catchment, *Water Resour. Res.*, *46*, W10502, doi:10.1029/2009WR008777.
- Tirone, G. (2003), Stima del bilancio del carbonio di due ecosistemi forestali Mediterranei. Confronto tra una lecceta e una pineta, PhD thesis, Dep. of For. Sci. and Resour., Univ. of Tuscia, Viterbo, Italy.
- Vachaud, G. A., S. A. Passerat, de, P. Balabanis, and M. Vauclin (1985), Temporal stability of spatially measured soil water probability density function, *Soil Sci. Soc. Am. J.*, *49*, 822–828, doi:10.2136/sssaj1985.03615995004900040006.
- Vanderlinden, K., H. Vereecken, H. Hardelauf, M. Herbst, G. Martinez, M. Cosh, and Y. Pachepsky (2012), Temporal stability of soil water contents: A review of data and analyses, *Vadose Zone J.*, *11*(4), doi:10.2136/vzj2011.0178.
- Vereecken, H., J. A. Huisman, H. R. Bogaen, J. Vanderborght, J. A. Vrugt, and J. W. Hopmans (2008), On the value of soil moisture measurements in vadose zone hydrology: A review, *Water Resour. Res.*, *44*, W00D06, doi:10.1029/2008WR006829.
- Vivoni, E. R., J. C. Rodríguez, and C. J. Watts (2010), On the spatiotemporal variability of soil moisture and evapotranspiration in a mountainous basin within the North American monsoon region, *Water Resources Res.*, *46*, W02509, doi:10.1029/2009WR008240.
- Wang, Y.-P., and R. Leuning (1998), A two-leaf model for canopy conductance, photosynthesis and partitioning of available energy. I. Model description and comparison with a multi-layered model, *Agric. For. Meteorol.*, *91*, 89–111.
- Western, A., S. Zhou, R. Grayson, T. McMahon, G. Blöschl, and D. Wilson (2004), Spatial correlation of soil moisture in small catchments and its relation to dominant spatial hydrological processes, *J. Hydrol.*, *286*, 113–134.
- Western, A. W., and G. Blöschl (1999), On the spatial scaling of soil moisture, *J. Hydrol.*, *217*, 203–224.
- Western, A. W., G. Blöschl, and R. B. Grayson (1998), Geostatistical characterisation of soil moisture patterns in the Tarrawarra catchment, *J. Hydrol.*, *205*, 20–37.
- Western, A. W., R. B. Grayson, G. Blöschl, G. R. Willgoose, and T. A. McMahon (1999), Observed spatial organization of soil moisture and its relation to terrain indices, *Water Resour. Res.*, *35*(3), 797–810.
- Wilson, D. J., A. W. Western, and R. B. Grayson (2004), Identifying and quantifying sources of variability in temporal and spatial soil moisture observations, *Water Resour. Res.*, *40*, W02507, doi:10.1029/2003WR002306.
- Xu, L., and D. D. Baldocchi (2004), Seasonal variation in carbon dioxide exchange over a Mediterranean annual grassland in California, *Agric. For. Meteorol.*, *1232*, 79–96, doi:10.1016/j.agrformet.2003.10.004.